

Water Resources Research®



RESEARCH ARTICLE

10.1029/2021WR031721

The Contribution of Transpiration to Precipitation Over African Watersheds

S. A. Te Wierik^{1,2} , J. Keune³ , D. G. Miralles³ , J. Gupta² , Y. A. Artzy-Randrup¹,
L. Gimeno⁴, R. Nieto⁴ , and L. H. Cammeraat¹ 

¹Institute for Biodiversity and Ecosystem Dynamics, University of Amsterdam, Amsterdam, The Netherlands, ²Governance and Inclusive Development, University of Amsterdam, Amsterdam, The Netherlands, ³Hydro-Climat Extremes Lab, Ghent University, Ghent, Belgium, ⁴Environmental Physics Laboratory (EPhysLab), Centro de Investigación Mariña, Universidade de Vigo, Vigo, Spain

Key Points:

- We show the contribution of transpiration to precipitation over 25 African watersheds based on satellite data and Lagrangian modeling
- Transpiration contributes to more than 50% of the precipitation over the African continent, although the variability among watersheds is large
- The Congo and Senegal show contrasting trends in precipitation, seemingly associated with different contributions of transpiration and oceanic evaporation

Supporting Information:

Supporting Information may be found in the online version of this article.

Correspondence to:

S. A. Te Wierik,
s.a.tewierik@uva.nl

Citation:

Te Wierik, S. A., Keune, J., Miralles, D. G., Gupta, J., Artzy-Randrup, Y. A., Gimeno, L., et al. (2022). The contribution of transpiration to precipitation over African watersheds. *Water Resources Research*, 58, e2021WR031721. <https://doi.org/10.1029/2021WR031721>

Received 30 NOV 2021

Accepted 9 OCT 2022

Author Contributions:

Conceptualization: S. A. Te Wierik, J. Keune

Formal analysis: S. A. Te Wierik, J. Keune

Funding acquisition: D. G. Miralles, J. Gupta, Y. A. Artzy-Randrup, L. H. Cammeraat

Methodology: S. A. Te Wierik, J. Keune

Project Administration: D. G. Miralles, J. Gupta, Y. A. Artzy-Randrup, L. H. Cammeraat

Resources: J. Keune, D. G. Miralles

Abstract The redistribution of biological (transpiration) and non-biological (interception loss, soil evaporation) fluxes of terrestrial evaporation via atmospheric circulation and precipitation is an important Earth system process. In vegetated ecosystems, transpiration dominates terrestrial evaporation and is thought to be crucial for regional moisture recycling and ecosystem functioning. However, the spatial and temporal variability in the dependency of precipitation on transpiration remains understudied, particularly in sparsely sampled regions like Africa. Here, we investigate how biological and non-biological sources of evaporation in Africa contribute to rainfall over the major watersheds in the continent. Our study is based on simulated atmospheric moisture trajectories derived from the Lagrangian model FLEXPART, driven by 1° resolution reanalysis data over 1981–2016. Using daily satellite-based fractions of transpiration over terrestrial evaporation, we isolate the contribution of vegetation to monthly rainfall. Furthermore, we highlight two watersheds (Congo and Senegal) for which we explore intra- and interannual variability of different precipitation sources, and where we find contrasting patterns of vegetation-sourced precipitation within and between years. Overall, our results show that almost 50% of the annual rainfall in Africa originates from transpiration, although the variability between watersheds is large (5%–68%). We conclude that, considering the current and projected patterns of land use change in Africa, a better understanding of the implications for continental-scale water availability is needed.

1. Introduction

Ecosystems around the world are coping with increasing water stress due to climate change and anthropogenic disturbance. Global warming intensifies the hydrological cycle through increasing evaporation rates and precipitation intensity (Ficklin et al., 2019; Westra et al., 2014). Furthermore, rising atmospheric carbon concentrations enhance plant productivity (leading to “global greening,” see Piao et al., 2020), affecting hydrology at local to global scales (Lu et al., 2016; Zeng et al., 2018). Meanwhile, anthropogenic disturbance through direct extraction of surface- and groundwater leads to a global overexploitation of water resources (Wada et al., 2010), while land cover change has affected a third of the global land area, mostly in the direction of reducing vegetation cover (Winkler et al., 2021). While studies indicate that the effects of land cover change on the continental water cycle may be buffered by shallow groundwater (Zipper et al., 2019), land cover change has led to a general loss in the capacity of ecosystems to capture and retain water (Gerten et al., 2005), and a reduced flux of terrestrial evaporation (E , often referred to as “evapotranspiration”) (Sterling et al., 2013). E is pivotal for the distribution of water on our planet, being a key contributor to precipitation (P) over land (Eltahir, 1998; Tuinenburg et al., 2020; Van Der Ent et al., 2010). It is estimated that globally, 70% of terrestrial E rains back over the continents (Tuinenburg et al., 2020), which amounts to 40% of the total terrestrial P (Van Der Ent et al., 2010). The importance of terrestrial moisture recycling varies both in time and space, with some regions being highly dependent on this “self-supplied” moisture (Holgate et al., 2020; Keys et al., 2014). In Amazonia, for instance, the contribution of local E is important to maintain forest stability and buffer against droughts. About 20% to 45% of P over Amazonia originates from the region itself (Burde et al., 2006; Staal et al., 2018; Trenberth, 1999). Similarly, in the Congo watershed, up to half of P derives from the watershed itself (Sorí et al., 2017; Tuinenburg et al., 2020). It should be noted that moisture recycling metrics are scale-dependent (see Section 3.3) and therefore not directly comparable. Estimates of seasonal variability are, however, highly uncertain, ranging from 25% to 83% of wet season P originating from the Congo region itself (Dyer et al., 2017; Worden et al., 2021). In temperate regions and drylands, the sign and magnitude of moisture recycling has been

© 2022 The Authors.

This is an open access article under the terms of the [Creative Commons Attribution-NonCommercial License](https://creativecommons.org/licenses/by-nc/4.0/), which permits use, distribution and reproduction in any medium, provided the original work is properly cited and is not used for commercial purposes.

Software: J. Keune
Supervision: J. Keune, D. G. Miralles, J. Gupta, Y. A. Artzy-Randrup, L. H. Cammeraat
Visualization: S. A. Te Wierik
Writing – original draft: S. A. Te Wierik
Writing – review & editing: S. A. Te Wierik, J. Keune, D. G. Miralles, J. Gupta, L. H. Cammeraat

less investigated than for tropical forests (Wierik et al., 2021), although some studies suggest the contribution of local E is equally crucial for P supply in these regions (Miralles et al., 2016; Nieto et al., 2006; Savenije, 1995; Yu et al., 2017). Beyond self-supplied P , studies show moisture recycling cascades spanning over continents (Staal et al., 2018; Zemp et al., 2014), complex networks of atmospheric moisture exchange between regions (Keune & Miralles, 2019; Keys et al., 2017), and spatial hydrological connectivity through atmospheric pathways that supply moisture to densely inhabited regions (de Vrese et al., 2016; Keys et al., 2018). The large variation in the estimations following precipitation recycling studies is partly explained by the methods used, ranging from isotope ratios (Gat, 1996; Zhao et al., 2019), to various models, such as bulk recycling models (Burde et al., 2006; Pokam et al., 2012) or Eulerian and Lagrangian transport models (e.g., Tuinenburg et al., 2020; Van Der Ent et al., 2010), often employing different input data (Tuinenburg & Staal, 2020).

The increasing availability and resolution of satellite observations, land surface models (LSMs), isotope data, and field measurements enables the disaggregation of E into its different components (Stoy et al., 2019). Broadly speaking, the terrestrial E flux can be partitioned into the direct evaporation from the soil surface, intercepted rainfall, and open water bodies (hereafter collectively referred to as “ E_d ”), and the biological flux of transpiration (hereafter “ E_t ”) (Miralles et al., 2020). In general, vegetation cover regulates E_d and E_t in two major ways. First, passively, by changing the water and energy balance at the land surface, that is, through effective rainfall partitioning (Crockford & Richardson, 2000), changing the radiation partitioning (He et al., 2014; Otto et al., 2011), rainfall interception (Horton, 1919), changes in leaf area index (LAI) (Wang et al., 2014), and modifying the water retention capacity of the soil (D’Odorico et al., 2007). Second, actively: through biophysically regulated stomatal conductance and root growth, vegetation modulates the magnitude and timing of E_t (Jarvis et al., 1976). A multitude of methods has been developed to disaggregate E , but estimations of the global contribution of E_t to terrestrial E are highly uncertain, with reported values ranging between 24% and 90% due to the variety of methods applied (Wei et al., 2017). In general, isotopic analyses appear to provide estimates that are at the high end of that range: for example, an analysis of isotopic data of rivers and lakes around the world led to an estimated contribution of 80%–90% of E_t to E (Jasechko et al., 2013). Yet, Good et al. (2015) estimated E_t to E to be only 64% based on global isotopic mass balance of the atmosphere and ocean. In contrast, LSM tend to provide lower estimates: for example, Wang-Erlandsson et al. (2014) analyzed global E partitioning using a hydrological LSM and found a 59% contribution of E_t to E . Remote sensing based approaches, on the other hand, vary widely in regards to the E_t to E ratio depending on the model used (Miralles et al., 2016). By combining various estimates for different vegetation types, Wei et al. (2017) presented a composite approach that suggested an average 57% contribution of global E_t to E . Regional differences in this ratio are expected to occur among different ecosystems and climates (Green et al., 2017; Miralles et al., 2016; Pranindita et al., 2021).

Although vegetation is considered a particularly important contributor to precipitable moisture (Meier et al., 2021; O’Connor et al., 2021), only few moisture recycling studies explicitly differentiate between biological and non-biological evaporation fluxes. Existing studies at the global level used partitioned E estimates from a LSM (Wang-Erlandsson et al., 2014), coupled to an atmospheric moisture tracking model, to estimate spatially distributed moisture recycling metrics (van der Ent et al., 2014), or applied a “green earth” and “desert earth” scenario to estimate the contribution of vegetation to global P (Keys et al., 2016). The former study estimated that 56% of global E_t returns to the land surface as P (van der Ent et al., 2014); the latter concluded that global vegetation cover regulates 20% of the total P over land. Based on several studies, a review paper from Schlesinger and Jasechko (2014) estimated that E_t accounts for 39% of terrestrial P through its contribution to precipitable atmospheric moisture. At the regional level, the direct contribution of vegetation to P through E_t is particularly poorly understood. Over Africa in particular, moisture recycling studies are sparse (Pokam et al., 2012), despite the current and future challenges posed by land use change, climate change and water scarcity in the region (Ahmadalipour et al., 2019; Haile et al., 2020; Held et al., 2005; Herrmann et al., 2020).

Considering the limited understanding of the dynamics of “vegetation-sourced P ,” as well as sparse moisture recycling assessments over Africa, this study has two objectives. First, to identify the contribution of vegetation-sourced P patterns over Africa, defined here as terrestrial P originating from E_t worldwide. We analyze the source regions of monthly P (over 1981–2016) for each of the 25 major African watersheds (sink regions) at 1° resolution. We use watersheds because they are a functional unit that is often used in hydrology. We distinguish between oceanic and terrestrial moisture sources, the latter disaggregated into terrestrial moisture sources from within the watershed (i.e., local moisture) and outside the watershed (i.e., remote moisture). Furthermore, we differentiate between E_t and E_d contributions to P . Second, to present and describe the development of a data

set following the analysis above; this data set is available online to spur further research on specific drivers and dynamics of moisture recycling over Africa (see Data Availability Statement). We use two watersheds (Congo and Senegal) to showcase some of the research possibilities offered by the available data. As such, we aim to contribute to enhanced understanding of the role of vegetation in the regional-to-continental water cycle and provide moisture recycling metrics for individual African watersheds.

2. Methodology

2.1. Data Generation: Identify Rainfall Source Regions Using FLEXPART

Our study is based on atmospheric moisture trajectories simulated with the Lagrangian model FLEXPART v9.01 (Stohl et al., 2005) and driven with ERA-Interim reanalysis data (e.g., Drumond et al., 2014; Nieto et al., 2019). The spatial resolution of the ERA-Interim forcing employed here is 1° , with 61 vertical levels between the land surface and 0.1 hPa (Dee et al., 2011). FLEXPART simulations are performed globally over 1981–2016 (36 years), initialized with a homogeneously distributed parcel density and 2 million parcels—on a 1° grid, this comprises approximately 30 parcels over each grid cell at each time step. While 3-hourly forecasts are used to supplement the 6-hourly reanalysis data to improve the accuracy of the simulated trajectory, only 6-hourly reanalysis time steps are used for the analysis. Simulations of FLEXPART driven with ERA-Interim reanalysis have been used in various studies (see, e.g., Table 1) and facilitate the identification of moisture fluxes with reasonable accuracy (Keune et al., 2022). While the use of higher-resolution forcing data sets may be desirable and promising (Hoffmann et al., 2019), moisture tracking studies that employ ERA-Interim as a forcing remain state-of-the-art for large-scale applications and have shown high agreements to other reanalyses, such as MERRA (Bosilovich et al., 2011) over the Western Sahel (Keys et al., 2014). Here, we evaluate moisture trajectories from FLEXPART over the 25 major African watersheds from HydroSHEDS (Lehner & Grill, 2013). Major watersheds were chosen to ensure that enough parcels can be tracked. For example, over the Senegal basin — one of the smaller basins that roughly comprises almost $5 \cdot 10^5 \text{ km}^2$ or $\sim 40 \text{ } 1^\circ \times 1^\circ$ grid cells—around $\sim 4,800$ parcels are evaluated each day. To estimate the origins of precipitation, we applied the moisture-tracking framework by (Keune et al., 2022) to the outputs from the FLEXPART simulations that are global in extent. The framework comprises three steps that are executed for each watershed over the full climatology: diagnosis, attribution, and bias-correction. A short description of each step is presented below; for details, see Keune et al. (2022).

First, daily fluxes of E and P over each 1° pixel are diagnosed by tracking changes in air parcel properties from the Lagrangian simulation using all global two-step trajectories (Keune et al., 2022). Here, the atmospheric moisture balance is used to estimate E and P from diagnosed changes in the specific humidity of air parcels, subjected to specific process-based detection criteria to filter for each process (diagnosis). Compared with observational reference data sets from MSWEP, OAFLUX, and GLEAM (Beck et al., 2019; Miralles et al., 2011; L. Yu & Weller, 2007), see description below, this evaluation of all parcels produces a data set representing accuracy and reliability that will be used in the third step (bias-correction). Second, in the attribution step, all air parcels arriving or residing over an individual watershed are selected and traced back for 15 days. Here, only precipitating parcels (i.e., parcels with relative humidity $>80\%$ losing moisture, following the convection parameterization from Emanuel (1991), are selected and their 15-day trajectories are evaluated to determine source–sink relationships of moisture. Note, however, that while we consider 15-day trajectories, the actual residence time of moisture in the atmosphere is not prescribed but determined through a discounting procedure at the parcel level (see, e.g., Sodemann et al., 2008; Läderach & Sodemann, 2016). Along each individual 15-day trajectory, all moisture gains occurring in the maximum atmospheric boundary layer between two time steps are considered to represent source locations associated with E ; we focus on the primary *surface* sources of precipitation only and neglect any secondary sources (such as re-evaporation in the atmosphere). Along each trajectory and between each identified surface source location and the P event, rain *en route* is accounted for through linear discounting (Sodemann et al., 2008) and ensures mass balance closure along the trajectories that are used to establish the source regions. The latter procedure assumes that the atmospheric boundary layer is well mixed, and it renders the prescription of the residence time unnecessary. Finally, in the third step, a daily bias-correction against observational data of E and P is performed using three observational reference datasets for each 1° grid cell (for source region E) and at the watershed level (for sink region P). As only primary source–sink relationships associated with surface fluxes E and sink fluxes P are considered, both fluxes can be bias-corrected using observational data (Keune et al., 2022). The absolute E flux in each source region pixel (as determined from in the diagnosis step

Table 1
Non-Exhaustive Overview of Moisture Recycling Studies Over the African Continent

Reference	Area	Main findings	Methods/models	Input data source
Savenije (1995)	Sahel	<ul style="list-style-type: none"> Moisture recycling in the Sahel account for 90% of the rainfall Irrigation during the dry season does not necessarily lead to increased precipitation due to low atmospheric vapor 	Simple linear analytical model based on Budyko (1974)	Rainfall gauges and runoff observations (field-based)
Gong and Eltahir (1996)	West Africa (5°N–15°N, 10°W–15°E)	<ul style="list-style-type: none"> Precipitation in West Africa derives for 23%, 27%, and 17% on evaporation from the Atlantic Ocean, West Africa and Central Africa, respectively Moisture supply from Central Africa is limited by the westerly monsoonal circulation 	Mass balance based on Budyko (1974)	ERA-40, 2.5°, daily, 1985–1995
Mohamed et al. (2005)	Nile Basin	<ul style="list-style-type: none"> Mean annual local moisture recycling of 11% 	Regional Atmospheric Climate Model (RACMO), applying Budyko framework, run for 35.96°N–12°S and 10°E–54.44°E, 0.44°	RCM initialized with ERA-40, 2.5°, 1995–2000Vegetation cover from GLCC GlobalLand Coverage CharacteristicsDischarge data (gauged measurements at 11 stations)Precipitation from ground stations; GPCC, 1°, monthly; FEWS, 0.1°
Los et al. (2006)	Sahel	<ul style="list-style-type: none"> Vegetation-rainfall feedback explains up to 30% of the rainfall variability between 15° and 20°N 	Statistical Vegetation Index Simulation (SVIS)	NDVI from AVHRR, 0.5°, monthly, 1982–1999Precipitation and temperature from CRU, 0.5°, monthly, 1901–2000
Van der Ent et al. (2010)	African continent	<ul style="list-style-type: none"> West-Africa is a major (precipitation) sink of continental evaporation Indian Ocean provides moisture to East and Central Africa, which in its turn provides moisture to West Africa Total precipitation from continental (terrestrial) origin over Africa = 49% 	Water accounting model	ERA-Interim, 1.5°, 6 hourly, 1998–2008
Pokam et al. (2012)	Equatorial Central Africa (5°N–5°S and 12.5°E–30°E)	<ul style="list-style-type: none"> Seasonal variability in moisture convergence determined by African Easterly Jet location and Atlantic Ocean Mean annual recycling ratio of 0.38 Low annual cycle/variability of recycling ratio 	2D bulk recycling model based on (Burde et al. (2006)	National Center for Environmental Prediction/ National Center for Atmospheric Research (NCEP/NCAR) Reanalysis, 1.9° and 2.5°, (monthly., at 1.9° × 1.9° and 2.5° × 2.5°)

Table 1
Continued

Reference	Area	Main findings	Methods/models	Input data source
Keys et al. (2014)	Western Sahel	<ul style="list-style-type: none"> Variation in Sahelian <i>E</i> most important to explain variance of precipitation 50.1% of the precipitation in the “core precipitation shed” derives from the land surface 	Eulerian Water Accounting Model 2 Layers (WAM-2Layers, v2.3.01),	ERA-Interim, 1.5° and MERRA, 1.0° × 1.25°, 1979–2013
Salih et al. (2015)	Sahelian Sudan	<ul style="list-style-type: none"> ITCZ is the main source of moisture During July and August, the ITCZ brings in half of the precipitation Despite being relatively dry, trade winds from the Arabian Peninsula are responsible for almost 30% of the precipitation 	FLEXPART v6.2	ERA-Interim, 1.5° and 2°, 3/6 hourly, 1998–2008
Miralles et al. (2016)	East and West Sudanian Savanna, Serengeti, Kalahari Desert	<ul style="list-style-type: none"> East Sudanian Savanna receives almost all <i>P</i> from terrestrial <i>E</i> Recycling ratio Kalahari Desert during growing season 34% Local recycling ratios increase during dry years (intensification of dry conditions) 	FLEXPART v9.0	ERA-Interim, Evaporation from GLEAM and OAFLUXVegetation Optical Depth (VOD), all data regridded to 0.25° with monthly time steps
Oguntunde et al. (2016)	Niger Basin	<ul style="list-style-type: none"> Local recycling between June and September amounts 21% 	Regional Climate Model (RegCM3) over 1981–2000	ERA-Interim Precipitation and temperature from CRU TS 2.1 (0.5°, monthly) River discharge from gauging stations
Dyer et al. (2017)	Congo Basin (10°S–5°N and 15°E–30°E)	<ul style="list-style-type: none"> Local <i>E</i> contribution varies between 24% and 38% throughout the year 	Water tagging capability in NCAR Community Earth System Model (CESM v1.2), run at 1.9° × 2.5° (30 vertical levels)	CRU, GPCP, ERA-Interim, and GPCC precipitation data sets
Sorí et al. (2017)	Congo Basin	<ul style="list-style-type: none"> The Congo Basin provides over 50% of the total atmospheric moisture for precipitation High oceanic <i>E</i> events are not directly linked to increased <i>P</i> over the basin Dry/wet years are associated with lower/higher local moisture contribution 	FLEXPART v9.0	Precipitation from CRU TS v3.23, 0.5° Runoff from GRDCEvaporation from GLEAM v2 and OAFLUXERA-Interim, 1°, 6 hourly
Yu et al. (2017)	Sahel	<ul style="list-style-type: none"> Oceanic forcing (i.e., SST) dominates precipitation variability (22% annual mean), except during post-monsoon period (SON) Annual mean terrestrial forcing of 8%, with 18% in SON 	A multivariate, lagged Generalized Equilibrium Feedback Assessment (GEFA)	Various land and ocean variables, see Yu et al. (2017) supplementary material for full overview

Table 1
Continued

Reference	Area	Main findings	Methods/models	Input data source
Keys and Wang-Erlandsson (2018)	Niger	<ul style="list-style-type: none"> 41% of annual precipitation derives from the ocean 9% derives from Niger itself, mostly from the South of the country 	WAM-2layers	ERA-Interim, 1.5°, 3/6 hourly
Wang-Erlandsson et al. (2018)	Congo Basin	<ul style="list-style-type: none"> Half of the streamflow in the Congo river is depending on terrestrial moisture recycling 	STEAM and WAM-2Layers	Meteorological data with ERA-Interim, 1.5°, 3/6 hourly, 1995–2014 Land Cover data with Ramankutty potential land-cover, IGBP (MCD1C1), MIRCA2000 v1.1 Precipitation from MSWEP v1, 0.25° regrided to 1.5° Runoff data from GRDC, 0.5° regrided to 1.5°
Notaro et al. (2019)	Sahel, Greater Horn of Africa, WAM-region, Congo basin	<ul style="list-style-type: none"> Land–atmosphere feedbacks are most prominent in semi-arid regions Forcing impact of soil moisture and vegetation is comparable of oceanic forcing for the whole region 	A multivariate Stepwise Generalized Equilibrium Feedback Assessment (SGEFA)	Various land surface variables, see Table 1 in Notaro et al. (2019) for full overview
Tuinenburg et al. (2020)	Congo basin	<ul style="list-style-type: none"> Evaporation recycling of 60% Precipitation recycling of 47% 	UTrack, analysis at 0.5°, monthly	ERA5, 0.25°, hourly, 2008–2017
Worden et al. (2021)	Congo basin	<ul style="list-style-type: none"> 83% of free tropospheric moisture comes from terrestrial E in February (first rain peak) During the second rain peak (September–October), only 31% derives from terrestrial E 	Statistical model based on satellite observations of deuterium content in water vapor	Deuterium content from NASA Tropospheric Emission Spectrometer; SIF from GOME-2 V26 740 nm data Precipitation from TRMM, 0.25° E from MODIS and ERA5, 0.25°, daily

above) is used to bias correct E in the source region (Keune et al., 2022); therefore, the relative contribution of each source pixel contribution over the absolute E flux in the same pixel is calculated, and bias-corrected over the ocean with OAFLUX (Yu & Weller, 2007), and over land using GLEAM v3.5a (Martens et al., 2017). P in the sink region (i.e., the watershed) is bias-corrected using MSWEP v2.2 (Beck et al., 2017, 2019). We apply MSWEP because it outperforms ERA-Interim P estimates over West and East Africa (Sahlu et al., 2017; Satgé et al., 2020). Moreover, Satgé et al. (2020) find that MSWEP best represents daily precipitation dynamics over West Africa compared to other precipitation data sets, such as CHIRPS (Funk et al., 2015). Considering the use of daily P fluxes in the analytical framework described above, we consider MSWEP most suited, despite limited capacity of earlier MSWEP versions (2.1) to represent regional hydroclimatic extremes and uncertainties over Africa (Awange et al., 2019). MSWEP is also used as input for GLEAM, which we expect to guarantee some water balance consistency.

Additionally, to unravel the contribution of E_s to P , we disaggregate the source contribution E in each grid cell into E_d and E_l based on daily E_d/E and E_l/E ratios from GLEAM, respectively. GLEAM estimates have been validated using eddy-covariance towers and in situ soil moisture measurements across the world (Martens et al., 2017) and have been used in several studies to benchmark other models (e.g., Dong et al., 2022; Lian et al., 2020). Chen

et al. (2022) find that GLEAM may overestimate E_p , especially during the wet season and in low vegetation cover regions. Nonetheless, Wei et al. (2017) show that GLEAM partitioning of evaporation and transpiration fluxes compares well to ensemble means and other global products. In short, the setup employed here tracks all precipitating parcels backwards and identifies all biological and non-biological moisture sources within the atmospheric boundary layer to establish the spatial source–sink relationships of moisture (Keune et al., 2022). The P data (in mm) is aggregated at the monthly level and is available from January 1981 up until December 2016 (see Data Availability Statement).

2.2. Data Analysis: Spatial and Temporal Variability of Moisture Source Regions

For each watershed, we analyze the mean monthly and mean annual contribution of five different moisture sources: oceanic E , local E_i and E_d , and remote E_i and E_d (Figure 1). We apply a global land surface mask to distinguish between ocean and terrestrial sources, use daily E_i and E_d fractions to distinguish between E_i and E_d fluxes (aggregated to monthly values), and employ watersheds from HydroSHEDS to distinguish between local and remote sources. Subsequently, based on individual watershed E_i contributions to P , we estimate the mean annual contribution of E_i to P (%) over the continent ($E_{i,c}$) as:

$$E_{i,c} = \frac{\sum_{i=1}^n \bar{P}_{i,i}}{\sum_{i=1}^n \bar{P}_i} \times 100$$

where \bar{P}_i is the mean annual rainfall ($\text{km}^3 \text{ year}^{-1}$) in watershed i ($n = 25$). We use flows (km^3) instead of fluxes (mm) to enable aggregation of the vegetation-sourced P contributions from all watersheds. Meanwhile, $\bar{P}_{i,i}$ is the \bar{P}_i originating from E_i ($\text{km}^3 \text{ yr}^{-1}$). Both \bar{P}_i and $\bar{P}_{i,i}$ represent the mean values over the full climatology (1981–2016).

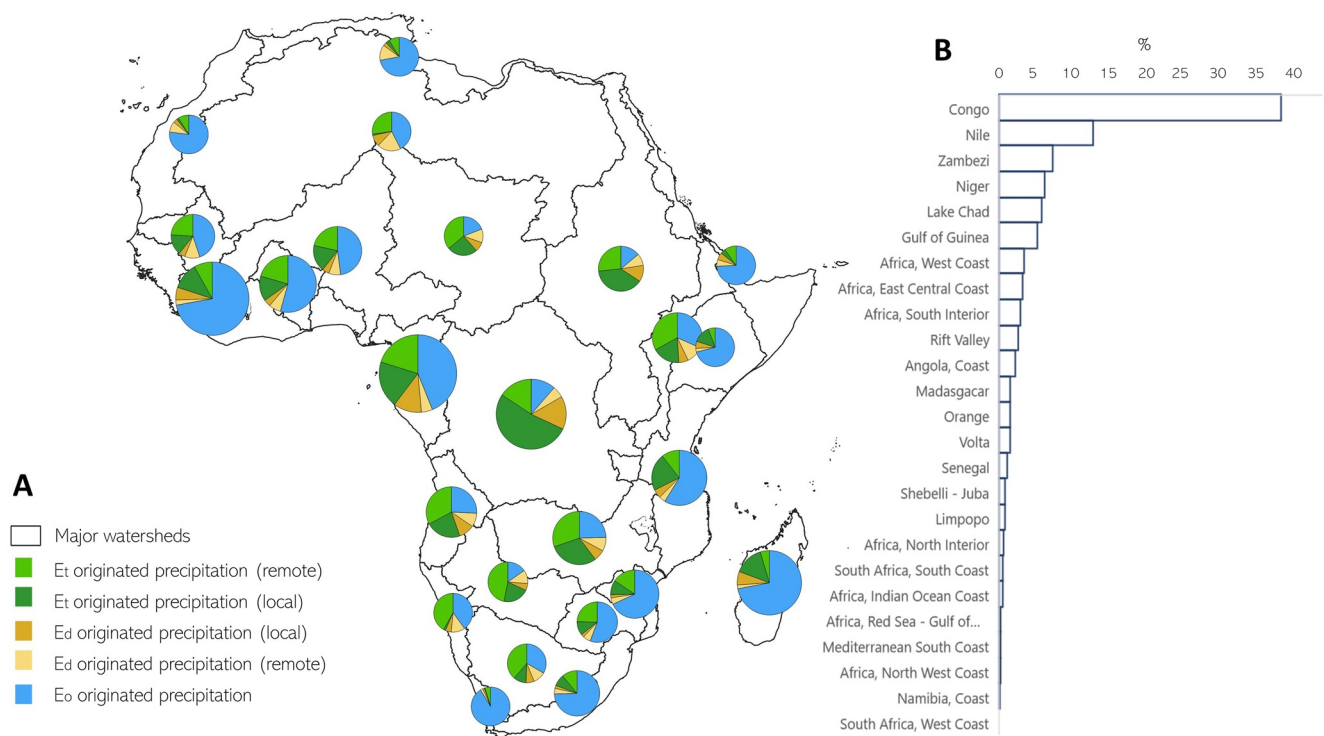


Figure 1. Sources of mean annual P over major African watersheds averaged over 1981–2016. (a) Shades of green represent vegetation-sourced P over the watershed; shades of yellow represent precipitation originated from E_p . Blue represents the ocean-originated precipitation. The size of each pie-chart represents the magnitude of mean annual precipitation. (b) Contribution (%) of each watershed to the total continental E_i -sourced precipitation. Figure S1 in Supporting Information S1 shows the corresponding names of the watersheds.

For each watershed, we distinguish between annual, wet season and dry season contributions of E_r . We identify wet (W_i) and dry (D_i) seasons for each watershed individually, based on mean monthly P for a particular month j being higher (wet season) or lower (dry season) than the mean monthly P for the whole record (\bar{P}_i), similar to the method to distinguish wet and dry years described by (Keys et al., 2018):

$$W_i \text{ if } \bar{P}_{j,i} > \bar{P}_i$$

and

$$D_i \text{ if } \bar{P}_{j,i} < \bar{P}_i,$$

where $\bar{P}_{j,i}$ represents the mean precipitation of a specific month j in watershed i , and \bar{P}_i the mean monthly precipitation in watershed i (mm year⁻¹). Both variables represent the mean values over the full climatology.

3. Results and Discussion

3.1. Variability of Rainfall Sources Over Major African Watersheds

Our results indicate that in most major African watersheds, a significant part of P is vegetation-sourced (Figure 1a). Overall, almost 50% of P over the African continent derives from transpiration worldwide (E_{tc}). This aligns with the 56% of global terrestrial P estimated to originate from E_t in van der Ent et al. (2014), but it is higher than the global estimate from Schlesinger and Jasechko (2014) of 39%. However, the latter is based on a data set that hardly sampled African regions. Figure 1b shows how much of the continental vegetation-sourced precipitation can be attributed to individual African watersheds and underlines the disproportionate contribution of the Congo basin.

The variability in annual E_t dependency between watersheds is large: between 5% and 68% of annual P is vegetation-sourced (Figure 2a). In most coastal watersheds along the Mediterranean and Southern Africa coast less than 20% of the annual P originates from E_r , as the majority derives from oceanic evaporation (Figure 1). In other regions, such as the tropical Congo basin, around 68% of the mean annual P derives from E_r , the majority (52%) originating from the watershed itself (Figure 1). In general, continental watersheds, such as Lake Chad and Zambezi, are more dependent on terrestrial E compared to oceanic E , with the majority of P originating from E_r .

During the dry season, the average dependency of P on E_t is slightly lower (Figure 2a). However, for some watersheds, E_t appears to be particularly important during the dry season. For example, in Senegal, the relative contribution of E_t to P increases from 36% during the wet season to 62% during the dry season (see Figure 2 and Figure S2 in Supporting Information S1)—indicating that vegetation is important to maintain the dry season P over the watershed. Overall, we find different seasonal dependency-regimes of vegetation-sourced P (Table 2) that may be influenced by land–atmosphere feedbacks coupled to seasonal climatic events (Green et al., 2017). For example, Yu et al. (2017) find that vegetation-rainfall linkages are exceptionally strong in the post-monsoon period over the Sahel. Furthermore, Pokam et al. (2012) show that seasonal cycles of moisture convergence, driven by the location of the African Easterly Jet, increase recycling ratio's in the dry season. For some regions, there is a constant contribution of E_t throughout the year (i.e., the difference of E_t contribution between the wet- and dry season <5%), whereas in other regions, E_t is particularly important in the dry (e.g., Senegal) or wet season (e.g., Namibia/Swakop). Figure 2 distinguishes between wet- and dry season E_t originating from local E_t and remote E_r . Some watersheds (e.g., Congo) show a strong dependency on local E_t throughout the year and rely little on other terrestrial source regions for both the dry and the wet season P . Other watersheds such as Zambezi and Lake Chad, which are in the vicinity of the Congo watershed, are dependent on remote E_t , which indicates that vegetation in the Congo is an important source for P in other watersheds (Van Der Ent et al., 2010).

3.2. Temporal Variability in the Congo and Senegal Watersheds

Table 2 highlights watersheds with a high (>30%) mean annual dependency on E_t for precipitation. The watersheds are described based on mean annual E_t dependence (%), interannual variability in E_t contribution using the coefficient of variation (COV, Figure S3 in Supporting Information S1), seasonal dependence on E_t (Figure 4 and Figure S2 in Supporting Information S1), and climatology (mean annual P in mm year⁻¹). Based on these criteria,

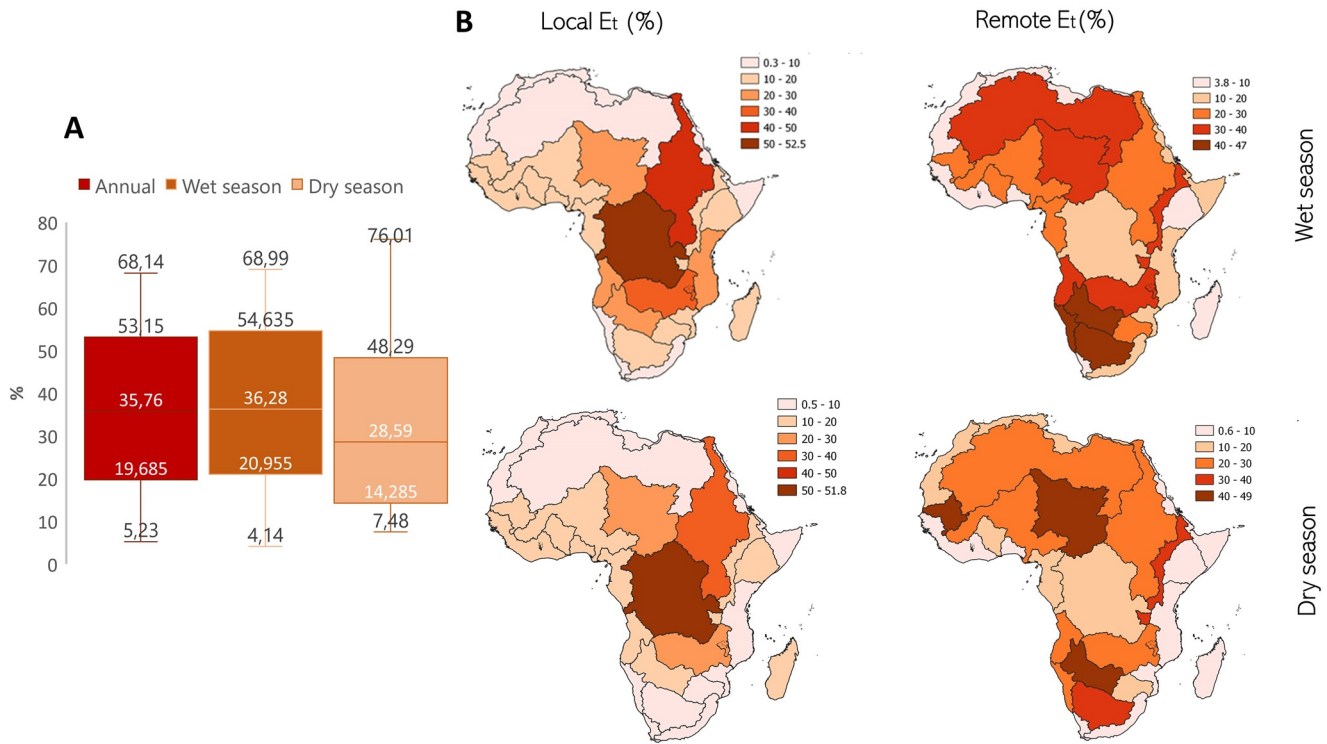


Figure 2. Seasonal variability of watersheds dependency on vegetation-sourced precipitation. (a) Variability in mean annual, wet season and dry season contribution of E_t to P between watersheds (note that numbers represent min, max, first quartile, median and third quartile). (b) Relative contribution of local E_t (left column) and remote E_t (right column) for the wet season (upper row) and dry season (lower row).

Table 2

List of Watersheds ($n = 12$) Where More Than 30% of the Mean Annual P Is Vegetation-Sourced (Mean Annual E_t Dependence in %)

Watershed	Mean annual E_t dependency (%)	Interannual variability vegetation-sourced P (COV)	Seasonal dependence on E_t (constant/wet/dry)	Mean annual P (mm year ⁻¹)
<i>Congo</i>	>50%	Low	Constant	1478
Nile	>50%	Low	Constant	614
Zambezi	>50%	High (dry season)	Wet season	853
Lake Chad	>50%	Moderate (dry season)	Dry season, terrestrial	370
Rift Valley	>50%	Low	Constant	757
Africa South Interior/Okavango	>50%	High (dry season)	Constant	476
<i>Senegal</i>	>30%	Moderate (dry season)	Dry season	575
Namibia/Swakop	>40%	High	Wet season	82
Orange	>40%	High (dry season)	Wet season	296
Africa East Central Coast	>40%	High (dry season)	Wet season (local)	923
Niger	>30%	Moderate (dry season)	Dry season (remote)	710
Gulf of Guinea	>30%	Low	Wet season	1814

Note. Interannual variability of vegetation-sourced P is defined here based on three value classes for the coefficient of variation: <20% (low); 20%–40% (moderate); and high (>40%). We distinguish between annual mean, wet and dry season. Seasonal dependence on E_t is based on the difference in relative contribution of E_t between the wet and dry season. To classify the watersheds based on the seasonal dependence, we use a threshold of 5% relative difference between the wet and dry seasons. It is considered constant if the difference between mean dry and wet season contribution <5%. The threshold value aims to standardize seasonal differences and is arbitrarily chosen. The watersheds in italic (*Congo* and *Senegal*) will be highlighted further.

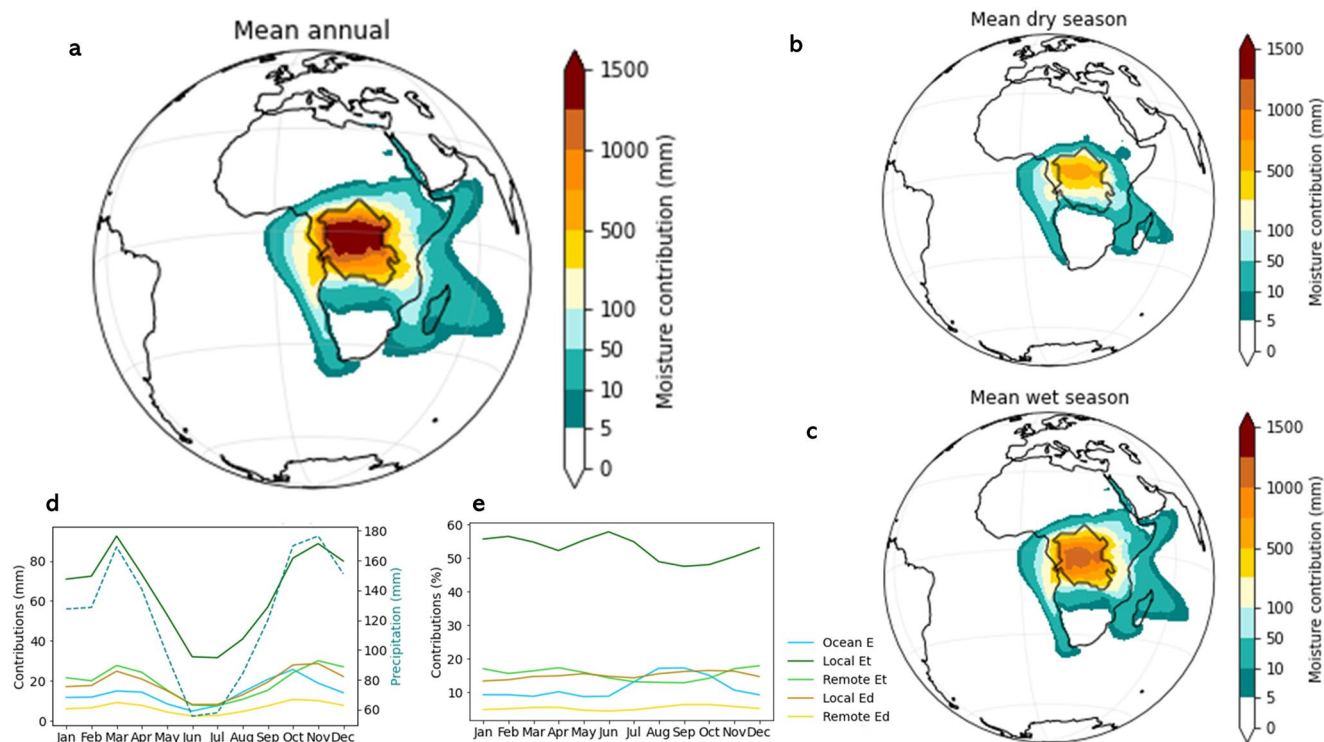


Figure 3. (a) Mean moisture source regions for the Congo watershed (black delineation). All moisture source regions <5 mm are considered insignificant contributors and are not visible on this map (in white); (b) Mean moisture source regions during the dry season (May–August); (c) Mean moisture source regions during the wet season (September–April); (d) Intra-annual absolute contributions of different moisture sources (mm, left axis) and P (mm, right axis, dashed line); (e) Intra-annual relative contributions of different moisture sources (%); all averaged over the full climatology.

we select two watersheds with a different hydro-climatology and describe their annual and seasonal source region characteristics in detail below: the Congo and Senegal watershed. Note that the spatially explicit source regions depicted in Figures 3 and 5 are defined based on “significant contributions” of grid cells that contribute (on average) more than 5 mm year^{-1} of E to P over the sink region (similar to the method applied by Keys et al. (2014).

3.2.1. Congo Watershed

The Congo watershed is one of the wettest watersheds in Africa (Table 1). It is located around the equator and covered by 2 million km^2 of tropical forest (Hansen et al., 2008). Our results indicate that most of the annual P is sourced from E from the watershed itself (68%) (Figure 3a). This is similar to the estimate from Sorí et al. (2017), who applied FLEXPART and ERA-Interim over 1980–2010 and found that, throughout the year, monthly P constitutes for 60% of E from the Congo itself. However, estimations from Tuinenburg et al. (2020) using the Lagrangian moisture tracking model UTrack (forced with ERA5) are substantially lower (47% of P derived from local E). Similarly, Dyer et al. (2017) apply a Eulerian moisture tracking scheme within a NCAR Community Earth System Model (CESM) over the Congo basin, but estimate that local E contribution varies between 24% and 38% throughout the year.

Only 11% of the mean annual P derives from the ocean, both the Indian Ocean on the east side of the continent, and the South Atlantic along the west coast. Despite the stable relative contributions of different moisture sources throughout the year (Figure 3e), there is a clear dip in the amount of P between May and August (i.e., the dry season), which corresponds to a reduction in the contribution of local E_i to rainfall (Figure 3d). Two distinct rainy seasons emerge in the boreal fall and spring (Figure 3d), which are associated with the passing of the inter-tropical convergence zone (Notaro et al., 2019). Overall, the relative contribution of local E_i to P is persistently high throughout the year (around 50%; Figure 3e). Further, even during the dry season, the absolute contribution of local vegetation-sourced P is dominant (Figure 3d), and the relative contribution is slightly increased (Figure 3e)—thus indicating that local vegetation maintains P over the Congo basin during the dry season even

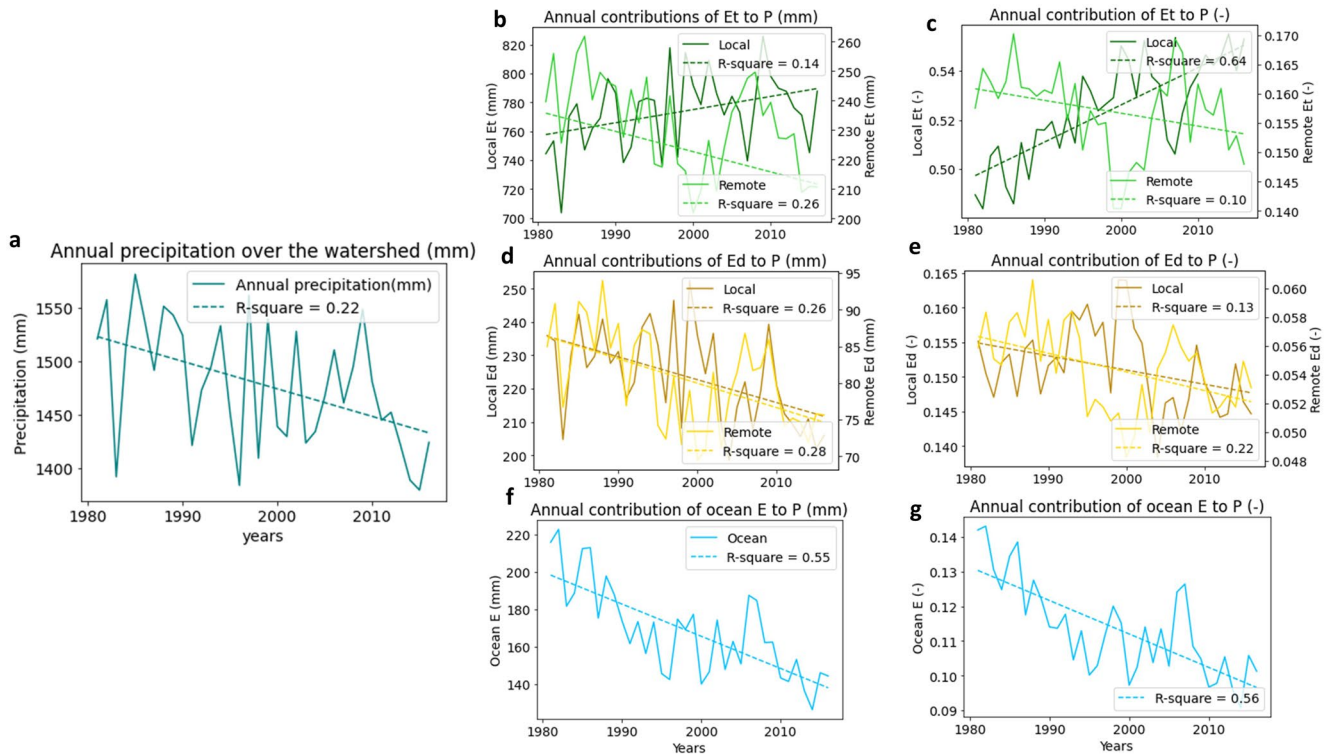


Figure 4. (a) Annual P (mm) over the Congo basin between 1981 and 2016. (b and c) Annual contribution of E_t to P in mm and fractional contribution to total rainfall, respectively. (d and e) Annual contribution of E_d in mm and fractional contribution to total rainfall, respectively. Full lines represents local sources, dashed line represents remote sources. (f and g) Annual contribution of oceanic E to P in mm and fractional contribution to total rainfall, respectively. Note the different scaling of the x -axes corresponding to local (left y -axis) and remote (right y -axis) sources of E_t and E_d contributions.

when oceanic moisture convergence is lower. In line with findings from Worden et al. (2021), increased advection of ocean air in the September–November rainy season slightly reduces the relative contribution from land E .

Addressing the changes in P and the contribution of different moisture sources between years (Figure 4), we observe three remarkable patterns. First, we find a decreasing trend in annual P (Figure 4a) as derived from MSWEP that seems to correspond primarily to decreasing oceanic moisture contributions (Figure 4f), in contrast to observed global trends of increasing ocean contributions (Findell et al., 2019), and as noted in previous studies (Gimeno, Nieto, & Sorí, 2020). Sorí et al. (2022) confirm a drying trend, particularly in the northern part of the Congo basin. A similar and persistent drying trend over the Congo was found by Cook et al. (2020) using multiple P data sets. They found reduced P over the Congo from 1979 onwards and explained this trend with shifting thermal lows that weaken moisture convergence in the (boreal) spring and fall; in the boreal summer, enhanced drying is associated with increasing warming over the Sahara (Cook et al., 2020) and an increasing length of the dry season (Jiang et al., 2019). Others have attributed the trends of observed drying over equatorial Africa (including the Congo) to the Atlantic Multidecadal Oscillation changing sea surface temperatures (SSTs) over the North Atlantic, warming over the Indian Ocean, and tropical biomass burning further causing increasing carbonaceous aerosol concentrations in the atmosphere (Diem et al., 2014). As such, drivers of observed P reductions remain debated. Second, our results indicate a slight increase in absolute and relative contributions of local E_t (Figures 4b and 4x) along with a reduction in E_d contributions to P (Figure 4d). The increasing relative contributions of local E_t is evident during both wet and dry seasons (Figure S4 in Supporting Information S1). This implies that contributions of local E_t to P increase, and vegetation-sourced E becomes more important for P over the Congo. This unexpected increase of vegetation-sourced P in light of an increasing drying trend may be explained by biological responses at the plant level. Asefi-Najafabady and Saatchi (2013) found that progressive drying had no particular effect on tropical tree cover, suggesting that forests have adapted gradually to increasing drought conditions. This could imply that forests accessing deeper groundwater can maintain transpiration when precipitation is low (Pranindita et al., 2021). Increased E_t may also result from increased plant density

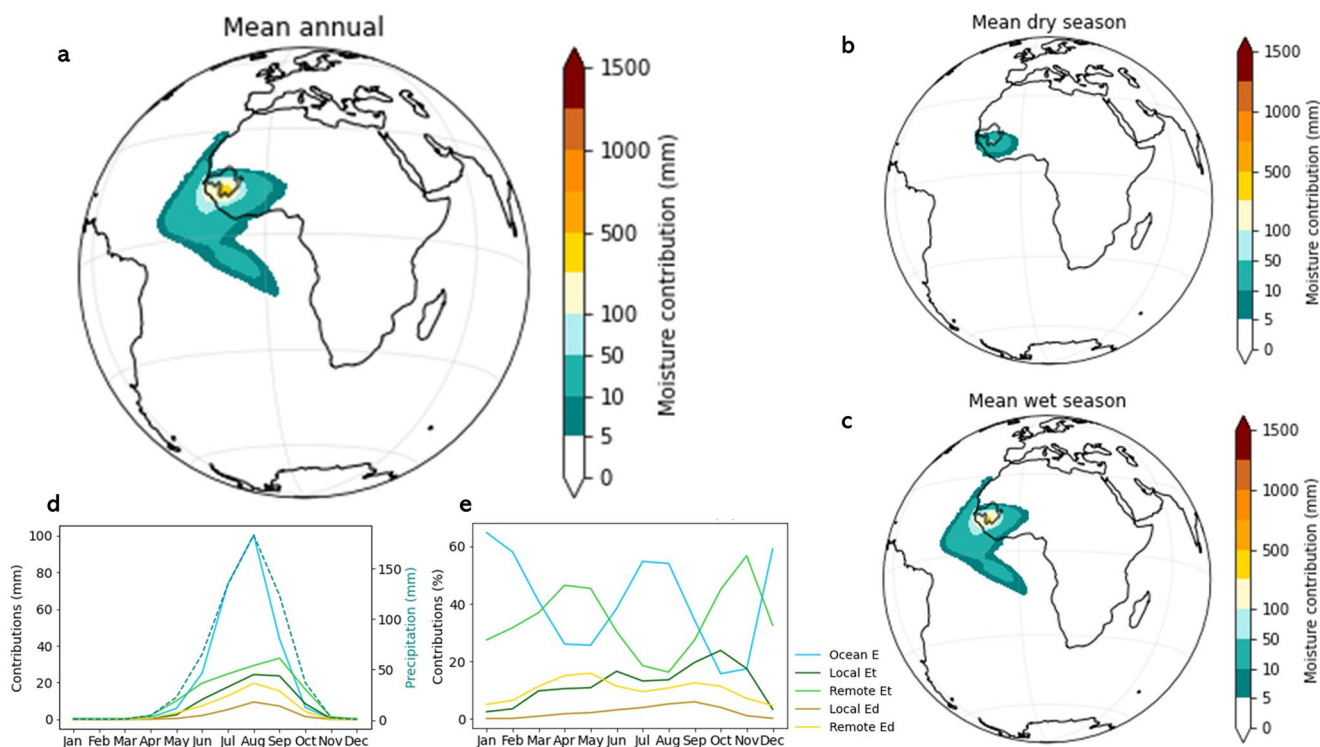


Figure 5. (a) Mean moisture source regions for the Senegal basin (black delineation). All moisture source regions <5 mm are considered insignificant contributors and are not visible on this map (in white); (b) Mean moisture source regions during the dry season; (c) Mean moisture source regions during the wet season; (d) Intra-annual absolute contributions of different moisture sources (mm, left axis) and P (mm, right axis, dashed line); (e) Intra-annual relative contributions of different moisture sources (%); all averaged over the full climatology.

with enhanced productivity. For example, Zeng et al. (2018) find that in response to rising atmospheric carbon concentrations (i.e., CO_2 fertilization), increasing LAI around the globe has led to increased evaporation and moisture recycling, particularly in wet regions. Nonetheless, the increasing E_t contributions are affected by the uncertainties in the GLEAM estimates of E_t and E_d , which are based on observed vegetation fractional cover and do not explicitly account for potential reductions in stomatal conductance in response to rising atmospheric CO_2 . Consequently, the contribution of local E for P trends over the Congo remains subject to debate (Dyer et al., 2017; Sorí et al., 2017; Worden et al., 2021). At last, we observe that around the year 2000, there is a reduction of both relative and absolute contribution of remote E_d and E_t (Figures 4b–4e) which may be explained by altered hydroclimatic conditions outside the Congo basin (Cook et al., 2020).

3.2.2. Senegal Watershed

The Senegal watershed is situated along the coast of West-Africa and receives a mean of 575 mm rainfall per year. On average, 39% of P is vegetation-sourced, with the majority coming from outside the basin (24% from remote E_t ; 15% from local E_t). Located in the Western Sahel and influenced by the West African Monsoon (WAM) (Niang et al., 2020; Nouaceur & Murarescu, 2020), the basin is characterized by a distinct wet and dry season (Figure 5d). On average, only 12% (70 mm) of the annual P falls during the dry season (November–April). More than half of that derives from E_t (Figure 5e). Most of P falls in the wet season (on average 505 mm between May and October). Although most wet season P originates from the ocean, E_t still constitutes 36% of P , which implies that vegetation plays an important role to produce rainfall even when oceanic influx is dominant. Moreover, remote vegetation supplies most of the moisture for P during the onset and cessation of the wet season (light green line in Figure 5e). The alternating importance of oceanic (blue line) and remote E_t sources (light green line) in Figure 5e may suggest the existence of a land–atmosphere feedback in the post-monsoon period to which vegetation-sourced P contributes significantly (Breil et al., 2017; Notaro et al., 2019).

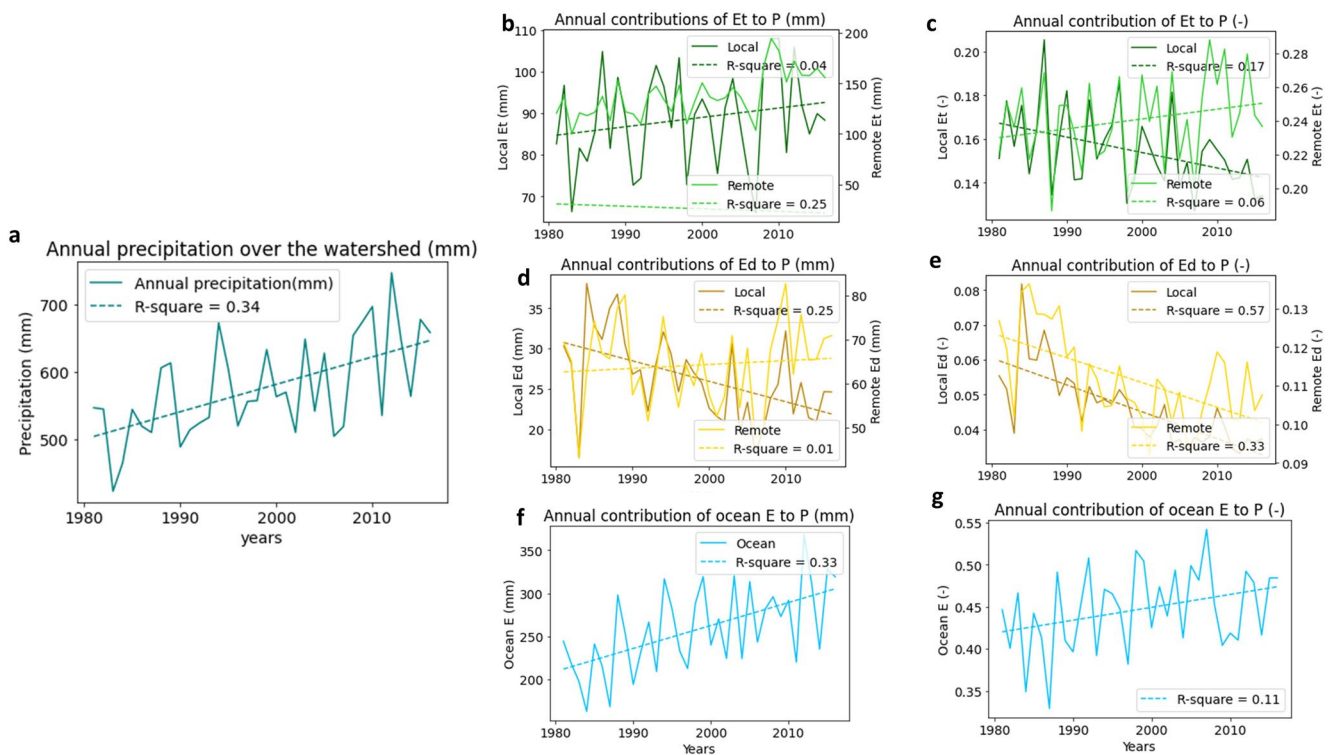


Figure 6. (a) Annual P (mm) over the Senegal basin between 1981 and 2016; (b and c) Annual contribution of E_v to P in mm and fractional contribution to total rainfall, respectively. Full line represents local sources, dashed line represents remote sources; (d and e) Annual contribution of E_d in mm and fractional contribution to total rainfall, respectively. Full line represents local sources, dashed line represents remote sources. (f and g) Annual contribution of ocean E to P in mm and fractional contribution to total rainfall, respectively. Note the different scaling of the x-axes corresponding to local (left y-axis) and remote (right y-axis) sources of E_v and E_d contributions.

Over the years, we find an increase in mean annual P between 1981 and 2016 (Figure 6a). Similar trends were observed in earlier studies (Bodian et al., 2020; Nicholson et al., 2018; Nouaceur & Murarescu, 2020) which found that annual P has been recovering since the Sahelian drought of the 1970s, and linked the recent increase in P to rising SST over the Atlantic Ocean (Nouaceur & Murarescu, 2020). Correspondingly, we find an increasing importance of oceanic sources for P over Senegal for this period, with increasing relative and absolute contributions from the ocean (Figures 6f and 6g). This is in contrast to the decreasing contribution of oceanic evaporation to P in the Congo basin (Figure 4f), but in line with global studies (Findell et al., 2019; Gimeno, Vázquez, et al., 2020) that suggest an increasing importance of ocean evaporation for terrestrial P in light of climate change on a global average. CMIP5 models assessing 21st century precipitation characteristics of the WAM under RCP4.5 emission scenario also show increased rainfall during the monsoon season due to increased moisture flux convergence and local recycling (Monerie et al., 2016), although the predicted rainfall increase may be weakened by human-induced land use and land cover change (Quesada et al., 2017). Furthermore, the importance of remote E_v seems to increase at the expense of local E_v (Figure 6c), although in terms of absolute contributions, both source contributions slightly increase over time (Figure 6b) and thus contribute to the wetting trend observed over the watershed (Figure 6a). At last, relative contributions of E_d sources appear to diminish (Figure 6e), although no clear trend appears in terms of absolute contribution (Figure 6d). Hence, the increase in oceanic evaporation sources seems the most significant driver of increasing rainfall patterns over the Senegal basin while being supported by an increasing contribution of vegetation-sourced E_v on rainfall.

3.3. Limitations

Despite the clear contribution of vegetation-sourced P over the African continent, the level of analysis at the watershed-scale applied here is likely to overlook regional variabilities. Considering the average size of the watersheds included in this study ($\sim 1.2 \cdot 10^6$ km²), spatial variability of rainfall and rainfall source regions within

watersheds is likely to be high, at least for large watersheds covering various bioclimatic zones. Besides issues of scale, there are three major limitations:

First, although the results presented here indicate the importance of E_t in the continental water cycle over Africa, there are limited options to validate precipitation sources (Keune et al., 2022). The lack of ground-based P data over Africa makes estimations and corrections of simulated rainfall patterns cumbersome (Washington et al., 2013). Yet, Sorí et al. (2017) applied a similar methodology—using FLEXPART moisture trajectories, driven by ERA-Interim—and used ground-based P and runoff measurements to construct the climatology for the Congo basin. They found a significant relationship between FLEXPART simulations and ground-based data. However, the use of various precipitation products in studies over the Congo basin have led to contrasting conclusions regarding moisture source regions (Dyer et al., 2017) and precipitation trends (Washington et al., 2013).

Second, differentiation of E is based on daily E_t/E_d ratios from GLEAM, despite the lack of consensus on the best performing E product in Africa (Burnett et al., 2020; Miralles et al., 2016). Local comparisons with ground-based flux-tower meteorological data show that GLEAM has a generally good performance compared to other E models (see, e.g., McCabe et al., 2016; Michel et al., 2016). Over Africa, recent experiments on the performance of GLEAM have not reached converging conclusions (Dembélé et al., 2020; Khosa et al., 2019; Majozi et al., 2017). GLEAM estimates are at the high end of E_t/E_d estimates (Wei et al., 2017), which implies that E_t contributions to P , as presented in this study, are more likely to be over-rather than underestimated.

Third, our presented moisture recycling metrics are strongly coupled to the choice of forcing and bias-correction data (i.e., ERA-Interim, OAFUX, MSWEP, and GLEAM), as well as the water accounting method applied (i.e., Lagrangian moisture tracking using FLEXPART). For example, Keune et al. (2022) studied the uncertainty inherent in the evaluation of Lagrangian trajectories; according to their analysis, the present study may yield moisture recycling ratios that are on the upper end of model-internal uncertainties. This finding is in line with other studies, using different datasets and models, and yielding lower moisture recycling estimates (see Table 1). However, as mentioned earlier, our results for the Congo align well with studies applying similar water accounting methods (Sorí et al., 2017), but are larger than those based on Eulerian frameworks (Dyer et al., 2017). Accordingly, the findings presented here are sensitive to the methodological choices, of which the strength and uncertainties could be addressed in further studies.

With respect to interpretations of the results, there are two major limitations. First, the overall P source regions show that vegetation-sourced P is substantial over the African continent, which is corroborated by other studies that investigate the role of vegetation cover in moisture recycling (Aemisegger et al., 2014; Miralles et al., 2016; O'Connor et al., 2021; van der Ent et al., 2014; Wang-Erlandsson et al., 2014; Zhao et al., 2019). Yet, these results cannot be directly used to infer the impact of land cover changes on P patterns. As also argued by Baudena et al. (2021), implicit assumptions of proportional change to P in response to changes in E_t imply a simplification. Changes in vegetation cover affect local coupling and atmospheric circulation via land-atmosphere feedbacks (Goessling & Reick, 2011)—which further influence moisture recycling dynamics. It remains unclear at which scale of land cover change this leads to certain effects on atmospheric circulation, although Lawrence and Vandecar (2015) suggest that a threshold for tropical deforestation exists at which rainfall is significantly reduced. Finally, the presented moisture recycling metrics are valid for individual watersheds, but are not comparable across watersheds, as the moisture recycling is per definition area-dependent: the whole Earth has a moisture recycling ratio of 1, whereas an infinitely small area would have a moisture recycling ratio close to zero (Trenberth, 1999). As such, larger watersheds are expected to have higher moisture recycling ratios.

4. Conclusion

This study sets out to assess the spatial and temporal variability of rainfall sources over major African watersheds and identify the role of vegetation in contributing to these patterns. Our analysis shows that, on average, almost 50% of the rainfall over Africa is vegetation-sourced, although the variation between watersheds is large: mostly coastal watersheds are predominantly dependent on oceanic evaporation, while many large inland watersheds—such as the Congo and Nile—show strong dependencies on vegetation-sourced precipitation. Whereas some watershed show dependency on vegetation-sourced precipitation year-round (i.e., Congo and Niger), others show large seasonal discrepancies (i.e., Senegal and Zambezi). The two watersheds featured in this study highlight these contrasting patterns. In the Congo basin, local E_t is a significant contributor to year-round P and also

appears to sustain precipitation in surrounding watersheds. For the Senegal basin, seasonally varying dependencies on remote E_i suggests the existence of a vegetation-feedback in the post-monsoon period. Interestingly, we find contrasting P trends that can be attributed to trends in moisture contributions from the ocean for the two basins: over Senegal, increased rainfall corresponds to increasing contributions of oceanic evaporation, possibly linked to observed SSTs over the Atlantic as suggested in previous studies. However, over the Congo, a persistent drying trend corresponds to reduced contributions of oceanic evaporation, and increased relative contributions of local E_i to sustain rainfall. As such, this suggests that local vegetation-sourced precipitation becomes increasingly important to sustain rainfall over the Congo. In light of rapid deforestation observed over Africa (FAO, 2020), it is crucial to understand how precipitation is affected by such interventions. The accompanying data set which this study presents can hence support further research on the contribution and importance of transpiration over different land cover types for rainfall trends and anomalies in the region.

Data Availability Statement

The data set supporting this manuscript (Te Wierik et al., 2022) is available via <https://figshare.com/s/4a40b-b2fe82b5db294c2>, in NetCDF files at 1° resolution for individual watersheds (monthly precipitation source regions over 1981–2016). This includes the accompanying code to process and visualize the precipitation source regions. The data can be cited as: (Te Wierik et al., 2022, Rainfall sources over African Watersheds, Dataset. <https://doi.org/10.6084/m9.figshare.17099888.v1>). Other data used in this study: HydroSHEDS are available via <https://data.apps.fao.org/catalog/iso/e54e2014-d23b-402b-8e73-c827628d17f4>; ERA-Interim data are available via <https://apps.ecmwf.int/datasets/>. GLEAM data are available via <https://www.gleam.eu/>; MSWEP data is available via <http://www.gloh2o.org/>. This publication is based upon the WHOI OaFlux datasets supported by the NOAA's Global Ocean Monitoring and Observing (GOMO) Program and NASA's Making Earth System Data Records for Use in Research Environments (MEAsURES) Program. OaFlux data as used here, is available from <https://oafux.whoi.edu/data-access/>. The framework for analysis of FLEXPART data (Keune et al., 2022) is available via <https://github.com/h-cel/hamster>.

Acknowledgments

S.W., J.G., Y.A., and E.C. are grateful to the Institute for Advanced Study (IAS) and Institute for Interdisciplinary Studies (IIS) from the University of Amsterdam, for providing the opportunity and support for this research through the Interdisciplinary Doctorate Agreement (IDA) of the University of Amsterdam. J.K. and D.G.M. acknowledge support from the European Research Council (ERC) under grant agreement 715254 (DRY-2-DRY) and the European Union H2020 project 869550 (DOWN2EARTH). J.K. is grateful for the support from the Research Foundation-Flanders (FWO) under grant 1244122N. R.N. and L.G. acknowledge the support by the LAGRIMA project (RTI2018-095772-B-I00) funded by the Ministerio de Ciencia, Innovación y Universidades, Spain. The computational resources and services used in this work were provided by the VSC (Flemish Supercomputer Center), funded by the FWO and the Flemish Government, Department of Economy, Science and Innovation (EWI). EPhysLab-UVigo is grateful for the support from the Xunta de Galicia (ED431C 2021/44, Programa de Consolidación e Estructuración de Unidades de Investigación Competitivas (Grupos de Referencia Competitiva) and Consellería de Cultura, Educación e Universidade).

References

- Aemisegger, F., Pfahl, S., Sodemann, H., Lehner, I., Seneviratne, S. I., & Wernli, H. (2014). Deuterium excess as a proxy for continental moisture recycling and plant transpiration. *Atmospheric Chemistry and Physics*, 14(8), 4029–4054. <https://doi.org/10.5194/acp-14-4029-2014>
- Ahmadalipour, A., Moradkhani, H., Castelletti, A., & Magliocca, N. (2019). Future drought risk in Africa: Integrating vulnerability, climate change, and population growth. *Science of the Total Environment*, 662, 672–686. <https://doi.org/10.1016/j.scitotenv.2019.01.278>
- Asefi-Najafabady, S., & Saatchi, S. (2013). Response of African humid tropical forests to recent rainfall anomalies. *Philosophical Transactions of the Royal Society B: Biological Sciences*, 368(1625), 20120306. <https://doi.org/10.1098/rstb.2012.0306>
- Awange, J. L., Hu, K. X., & Khaki, M. (2019). The newly merged satellite remotely sensed, gauge and reanalysis-based Multi-Source Weighted-Ensemble Precipitation: Evaluation over Australia and Africa (1981–2016). *Science of the Total Environment*, 670, 448–465. <https://doi.org/10.1016/j.scitotenv.2019.03.148>
- Baudena, M., Tuinenburg, O. A., Ferdinand, P. A., & Staal, A. (2021). Effects of land-use change in the Amazon on precipitation are likely underestimated. *Global Change Biology*, 27(21), 5580–5587. <https://doi.org/10.1111/gcb.15810>
- Beck, H. E., Vergopolan, N., Pan, M., Levizzani, V., van Dijk, A. I. J. M., Weedon, G. P., et al. (2017). Global-scale evaluation of 22 precipitation datasets using gauge observations and hydrological modeling. *Hydrology and Earth System Sciences*, 21(12), 6201–6217. <https://doi.org/10.5194/hess-21-6201-2017>
- Beck, H. E., Wood, E. F., Pan, M., Fisher, C. K., Miralles, D. G., van Dijk, A. I. J. M., et al. (2019). MSWEP V2 global 3-hourly 0.1° precipitation: Methodology and quantitative assessment. *Bulletin of the American Meteorological Society*, 100(3), 473–500. <https://doi.org/10.1175/BAMS-D-17-0138.1>
- Bodian, A., Diop, L., Panthou, G., Dacosta, H., Deme, A., Dezetter, A., et al. (2020). Recent trend in hydroclimatic conditions in the Senegal River Basin. *Water*, 12(2), 436. <https://doi.org/10.3390/w12020436>
- Bosilovich, M. G., Robertson, F. R., & Chen, J. (2011). Global energy and water budgets in MERRA. *Journal of Climate*, 24(22), 5721–5739. <https://doi.org/10.1175/2011JCLI4175.1>
- Breil, M., Panitz, H.-J., & Schädler, G. (2017). Impact of soil-vegetation-atmosphere interactions on the spatial rainfall distribution in the Central Sahel. *Meteorologische Zeitschrift*, 26(4), 379–389. Scopus. <https://doi.org/10.1127/metz/2017/0819>
- Budyko, M. I. (1974). *Climate and life*. Academic Press. Retrieved from https://scholar.google.com/scholar_lookup?title=Climate+and+life%26author=Budyko%2C+M.+I.+%26Mikhail+Ivanovich%29%26publication_year=1974
- Burde, G. I., Gandush, C., & Bayarjargal, Y. (2006). Bulk recycling models with incomplete vertical mixing. Part II: Precipitation recycling in the Amazon basin. *Journal of Climate*, 19(8), 1473–1489. <https://doi.org/10.1175/JCLI3688.1>
- Burnett, M. W., Quetin, G. R., & Konings, A. G. (2020). Data-driven estimates of evapotranspiration and its controls in the Congo Basin. *Hydrology and Earth System Sciences*, 24(8), 4189–4211. <https://doi.org/10.5194/hess-24-4189-2020>
- Chen, H., Zhu, G., Shang, S., Qin, W., Zhang, Y., Su, Y., et al. (2022). Uncertainties in partitioning evapotranspiration by two remote sensing-based models. *Journal of Hydrology*, 604, 127223. <https://doi.org/10.1016/j.jhydrol.2021.127223>
- Cook, K. H., Liu, Y., & Vizy, E. K. (2020). Congo Basin drying associated with poleward shifts of the African thermal lows. *Climate Dynamics*, 54(1), 863–883. <https://doi.org/10.1007/s00382-019-05033-3>

- Crockford, R. H., & Richardson, D. P. (2000). Partitioning of rainfall into throughfall, stemflow and interception effect of forest type, ground cover and climate. *Hydrological Processes*, *14*(16–17), 2903–2920. Scopus. [https://doi.org/10.1002/1099-1085\(200011/12\)14:16/17<2903::AID-HYP126>3.0.CO;2-6](https://doi.org/10.1002/1099-1085(200011/12)14:16/17<2903::AID-HYP126>3.0.CO;2-6)
- Dee, D. P., Uppala, S. M., Simmons, A. J., Berrisford, P., Poli, P., Kobayashi, S., & Andrae, U. (2011). The ERA-Interim reanalysis: Configuration and performance of the data assimilation system. *Quarterly Journal of the Royal Meteorological Society*, *137*(656), 553–597. <https://doi.org/10.1002/qj.828>
- Dembélé, M., Ceperley, N., Zwart, S. J., Salvatore, E., Mariethoz, G., & Schaeffli, B. (2020). Potential of satellite and reanalysis evaporation datasets for hydrological modelling under various model calibration strategies. *Advances in Water Resources*, *143*, 103667. Scopus. <https://doi.org/10.1016/j.advwatres.2020.103667>
- de Vrese, P., Hagemann, S., & Claussen, M. (2016). Asian irrigation, African rain: Remote impacts of irrigation. *Geophysical Research Letters*, *43*(8), 3737–3745. <https://doi.org/10.1002/2016GL068146>
- Diem, J. E., Ryan, S. J., Hartter, J., & Palace, M. W. (2014). Satellite-based rainfall data reveal a recent drying trend in central equatorial Africa. *Climatic Change*, *126*(1), 263–272. <https://doi.org/10.1007/s10584-014-1217-x>
- D’Odonico, P., Caylor, K., Okin, G. S., & Scanlon, T. M. (2007). On soil moisture–vegetation feedbacks and their possible effects on the dynamics of dryland ecosystems. *Journal of Geophysical Research*, *112*(G4). <https://doi.org/10.1029/2006JG000379>
- Dong, J., Lei, F., & Crow, W. T. (2022). Land transpiration–evaporation partitioning errors responsible for modeled summertime warm bias in the central United States. *Nature Communications*, *13*(1), 336. <https://doi.org/10.1038/s41467-021-27938-6>
- Drumond, A., Marengo, J., Ambrizzi, T., Nieto, R., Moreira, L., & Gimeno, L. (2014). The role of the Amazon basin moisture in the atmospheric branch of the hydrological cycle: A Lagrangian analysis. *Hydrology and Earth System Sciences*, *18*(7), 2577–2598. <https://doi.org/10.5194/hess-18-2577-2014>
- Dyer, E. L. E., Jones, D. B. A., Nusbaumer, J., Li, H., Collins, O., Vettoretti, G., & Noone, D. (2017). Congo Basin precipitation: Assessing seasonality, regional interactions, and sources of moisture. *Journal of Geophysical Research: Atmospheres*, *122*(13), 6882–6898. <https://doi.org/10.1002/2016JD026240>
- Eltahir, E. A. B. (1998). A soil moisture–rainfall feedback mechanism: I. Theory and observations. *Water Resources Research*, *34*(4), 765–776. <https://doi.org/10.1029/97WR03499>
- Emanuel, K. A. (1991). A scheme for representing cumulus convection in large-scale models. *Journal of the Atmospheric Sciences*, *48*(21), 2313–2329. [https://doi.org/10.1175/1520-0469\(1991\)048<2313:ASFRCC>2.0.CO;2](https://doi.org/10.1175/1520-0469(1991)048<2313:ASFRCC>2.0.CO;2)
- FAO. (2020). *Global forest resources assessment 2020*. FAO. <https://doi.org/10.4060/ca8753en>
- Ficklin, D. L., Abatzoglou, J. T., & Novick, K. A. (2019). A new perspective on terrestrial hydrologic intensity that incorporates atmospheric water demand. *Geophysical Research Letters*, *46*(14), 8114–8124. <https://doi.org/10.1029/2019GL084015>
- Findell, K. L., Keys, P. W., van der Ent, R. J., Lintner, B. R., Berg, A., & Krasting, J. P. (2019). Rising temperatures increase importance of oceanic evaporation as a source for continental precipitation. *Journal of Climate*, *32*(22), 7713–7726. <https://doi.org/10.1175/JCLI-D-19-0145.1>
- Funk, C., Peterson, P., Landsfeld, M., Pedreros, D., Verdin, J., Shukla, S., et al. (2015). The climate hazards infrared precipitation with stations—A new environmental record for monitoring extremes. *Scientific Data*, *2*(1), 150066. <https://doi.org/10.1038/sdata.2015.66>
- Gat, J. R. (1996). Oxygen and hydrogen isotopes in the hydrologic cycle. *Annual Review of Earth and Planetary Sciences*, *24*(1), 225–262. <https://doi.org/10.1146/annurev.earth.24.1.225>
- Gerten, D., Hoff, H., Bondeau, A., Lucht, W., Smith, P., & Zaehle, S. (2005). Contemporary “green” water flows: Simulations with a dynamic global vegetation and water balance model. *Physics and Chemistry of the Earth*, *30*(6), 334–338. <https://doi.org/10.1016/j.pce.2005.06.002>
- Gimeno, L., Nieto, R., & Sorí, R. (2020). The growing importance of oceanic moisture sources for continental precipitation. *Npj Climate and Atmospheric Science*, *3*(1), 1–9. <https://doi.org/10.1038/s41612-020-00133-y>
- Gimeno, L., Vázquez, M., Eiras-Barca, J., Sorí, R., Stojanovic, M., Algarra, I., et al. (2020). Recent progress on the sources of continental precipitation as revealed by moisture transport analysis. *Earth-Science Reviews*, *201*, 103070. <https://doi.org/10.1016/j.earscirev.2019.103070>
- Goessling, H. F., & Reick, C. H. (2011). What do moisture recycling estimates tell us? Exploring the extreme case of non-evaporating continents. *Hydrology and Earth System Sciences*, *15*(10), 3217–3235. Scopus. <https://doi.org/10.5194/hess-15-3217-2011>
- Gong, C., & Eltahir, E. (1996). Sources of moisture for rainfall in West Africa. *Water Resources Research*, *32*(10), 3115–3121. <https://doi.org/10.1029/96WR01940>
- Good, S. P., Noone, D., & Bowen, G. (2015). Hydrologic connectivity constrains partitioning of global terrestrial water fluxes. *Science*, *349*(6244), 175–177. <https://doi.org/10.1126/science.aaa5931>
- Green, J. K., Konings, A. G., Alemohammad, S. H., Berry, J., Entekhabi, D., Kolassa, J., et al. (2017). Regionally strong feedbacks between the atmosphere and terrestrial biosphere. *Nature Geoscience*, *10*(6), 410–414. <https://doi.org/10.1038/ngeo2957>
- Haile, G. G., Tang, Q., Hosseini-Moghari, S.-M., Liu, X., Gebremicael, T. G., Leng, G., et al. (2020). Projected impacts of climate change on drought patterns over East Africa. *Earth’s Future*, *8*(7), e2020EF001502. <https://doi.org/10.1029/2020EF001502>
- Hansen, M. C., Roy, D. P., Lindquist, E., Adusei, B., Justice, C. O., & Altstatt, A. (2008). A method for integrating MODIS and Landsat data for systematic monitoring of forest cover and change in the Congo Basin. *Remote Sensing of Environment*, *112*(5), 2495–2513. <https://doi.org/10.1016/j.rse.2007.11.012>
- He, T., Liang, S., & Song, D.-X. (2014). Analysis of global land surface albedo climatology and spatial-temporal variation during 1981–2010 from multiple satellite products. *Journal of Geophysical Research: Atmospheres*, *119*(17), 10281–10298. <https://doi.org/10.1002/2014JD021667>
- Held, I. M., Delworth, T. L., Lu, J., Findell, K. L., & Knutson, T. R. (2005). Simulation of Sahel drought in the 20th and 21st centuries. *Proceedings of the National Academy of Sciences*, *102*(50), 17891–17896. <https://doi.org/10.1073/pnas.0509057102>
- Herrmann, S. M., Brandt, M., Rasmussen, K., & Fensholt, R. (2020). Accelerating land cover change in West Africa over four decades as population pressure increased. *Communications Earth & Environment*, *1*(1), 1–10. <https://doi.org/10.1038/s43247-020-00053-y>
- Hoffmann, L., Günther, G., Li, D., Stein, O., Wu, X., Griessbach, S., et al. (2019). From ERA-Interim to ERA5: The considerable impact of ECMWF’s next-generation reanalysis on Lagrangian transport simulations. *Atmospheric Chemistry and Physics*, *19*(5), 3097–3124. <https://doi.org/10.5194/acp-19-3097-2019>
- Holgate, C. M., Evans, J., Dijk, A. V., Pitman, A. J., & Virgilio, G. (2020). Australian precipitation recycling and evaporative source regions. <https://doi.org/10.1175/jcli-d-19-0926.1>
- Horton, R. E. (1919). Rainfall interception. *Monthly Weather Review*, *47*(9), 603–623. [https://doi.org/10.1175/1520-0493\(1919\)47<603:RI>2.0.CO;2](https://doi.org/10.1175/1520-0493(1919)47<603:RI>2.0.CO;2)
- Jarvis, P. G., Monteith, J. L., & Weatherley, P. E. (1976). The interpretation of the variations in leaf water potential and stomatal conductance found in canopies in the field. *Philosophical Transactions of the Royal Society of London B Biological Sciences*, *273*(927), 593–610. <https://doi.org/10.1098/rstb.1976.0035>

- Jasechko, S., Sharp, Z. D., Gibson, J. J., Birks, S. J., Yi, Y., & Fawcett, P. J. (2013). Terrestrial water fluxes dominated by transpiration. *Nature*, 496(7445), 347–350. <https://doi.org/10.1038/nature11983>
- Jiang, Y., Zhou, L., Tucker, C. J., Raghavendra, A., Hua, W., Liu, Y. Y., & Joiner, J. (2019). Widespread increase of boreal summer dry season length over the Congo rainforest. *Nature Climate Change*, 9(8), 617–622. <https://doi.org/10.1038/s41558-019-0512-y>
- Keune, J., & Miralles, D. G. (2019). A precipitation recycling network to assess freshwater vulnerability: Challenging the watershed convention. *Water Resources Research*, 55(11), 9947–9961. <https://doi.org/10.1029/2019WR025310>
- Keune, J., Schumacher, D. L., & Miralles, D. G. (2022). A unified framework to estimate the origins of atmospheric moisture and heat using Lagrangian models. *Geoscientific Model Development*, 15(5), 1875–1898. <https://doi.org/10.5194/gmd-15-1875-2022>
- Keys, P. W., Barnes, E. A., Van Der Ent, R. J., & Gordon, L. J. (2014). Variability of moisture recycling using a precipitation shed framework. *Hydrology and Earth System Sciences*, 18(10), 3937–3950. Scopus. <https://doi.org/10.5194/hess-18-3937-2014>
- Keys, P. W., & Wang-Erlandsson, L. (2018). On the social dynamics of moisture recycling. *Earth System Dynamics*, 9(2), 829–847. Scopus. <https://doi.org/10.5194/esd-9-829-2018>
- Keys, P. W., Wang-Erlandsson, L., & Gordon, L. J. (2016). Revealing invisible water: Moisture recycling as an ecosystem service. *PLoS One*, 11(3), e0151993. <https://doi.org/10.1371/journal.pone.0151993>
- Keys, P. W., Wang-Erlandsson, L., & Gordon, L. J. (2018). Megacity precipitation sheds reveal tele-connected water security challenges. *PLoS One*, 13(3), e0194311. Scopus. <https://doi.org/10.1371/journal.pone.0194311>
- Keys, P. W., Wang-Erlandsson, L., Gordon, L. J., Galaz, V., & Ebbesson, J. (2017). Approaching moisture recycling governance. *Global Environmental Change*, 45, 15–23. Scopus. <https://doi.org/10.1016/j.gloenvcha.2017.04.007>
- Khosa, F. V., Feig, G. T., van der Merwe, M. R., Mateyisi, M. J., Mudau, A. E., & Savage, M. J. (2019). Evaluation of modeled actual evapotranspiration estimates from a land surface, empirical and satellite-based models using in situ observations from a South African semi-arid savanna ecosystem. *Agricultural and Forest Meteorology*, 279, 107706. Scopus. <https://doi.org/10.1016/j.agrformet.2019.107706>
- Läderach, A., & Sodemann, H. (2016). A revised picture of the atmospheric moisture residence time. *Geophysical Research Letters*, 43(2), 924–933. <https://doi.org/10.1002/2015GL067449>
- Lawrence, D., & Vandecar, K. (2015). Effects of tropical deforestation on climate and agriculture. *Nature Climate Change*, 5(1), 27–36. <https://doi.org/10.1038/nclimate2430>
- Lehner, B., & Grill, G. (2013). Global river hydrography and network routing: Baseline data and new approaches to study the world's large river systems. *Hydrological Processes*, 27(15), 2171–2186. <https://doi.org/10.1002/hyp.9740>
- Lian, X., Piao, S., Li, L. Z. X., Li, Y., Huntingford, C., Ciais, P., et al. (2020). Summer soil drying exacerbated by earlier spring greening of northern vegetation. *Science Advances*, 6(1), eaax0255. <https://doi.org/10.1126/sciadv.aax0255>
- Los, S. O., Weedon, G. P., North, P. R. J., Kaduk, J. D., Taylor, C. M., & Cox, P. M. (2006). An observation-based estimate of the strength of rainfall-vegetation interactions in the Sahel. *Geophysical Research Letters*, 33(16), L16402. <https://doi.org/10.1029/2006GL027065>
- Lu, X., Wang, L., & McCabe, M. F. (2016). Elevated CO₂ as a driver of global dryland greening. *Scientific Reports*, 6(1), 20716. <https://doi.org/10.1038/srep20716>
- Majazi, N. P., Mannaerts, C. M., Ramoelo, A., Mathieu, R., Mudau, A. E., & Verhoef, W. (2017). An intercomparison of satellite-based daily evapotranspiration estimates under different eco-climatic regions in South Africa. *Remote Sensing*, 9(4), 307. Scopus. <https://doi.org/10.3390/rs9040307>
- Martens, B., Miralles, D. G., Lievens, H., Van Der Schalie, R., De Jeu, R. A. M., Fernández-Prieto, D., et al. (2017). GLEAM v3: Satellite-based land evaporation and root-zone soil moisture. *Geoscientific Model Development*, 10(5), 1903–1925. Scopus. <https://doi.org/10.5194/gmd-10-1903-2017>
- McCabe, M. F., Ershadi, A., Jimenez, C., Miralles, D. G., Michel, D., & Wood, E. F. (2016). The GEWEX LandFlux project: Evaluation of model evaporation using tower-based and globally gridded forcing data. *Geoscientific Model Development*, 9(1), 283–305. <https://doi.org/10.5194/gmd-9-283-2016>
- Meier, R., Schwaab, J., Seneviratne, S. I., Sprenger, M., Lewis, E., & Davin, E. L. (2021). Empirical estimate of forestation-induced precipitation changes in Europe. *Nature Geoscience*, 14(7), 473–478. <https://doi.org/10.1038/s41561-021-00773-6>
- Michel, D., Jiménez, C., Miralles, D. G., Jung, M., Hirschi, M., Ershadi, A., et al. (2016). The WACMOS-ET project – Part 1: Tower-scale evaluation of four remote-sensing-based evapotranspiration algorithms. *Hydrology and Earth System Sciences*, 20(2), 803–822. <https://doi.org/10.5194/hess-20-803-2016>
- Miralles, D. G., Brutsaert, W., Dolman, A. J., & Gash, J. H. (2020). On the use of the term “evapotranspiration. *Water Resources Research*, 56(11), e2020WR028055. <https://doi.org/10.1029/2020WR028055>
- Miralles, D. G., De Jeu, R. A. M., Gash, J. H., Holmes, T. R. H., & Dolman, A. J. (2011). Magnitude and variability of land evaporation and its components at the global scale. *Hydrology and Earth System Sciences*, 15(3), 967–981. <https://doi.org/10.5194/hess-15-967-2011>
- Miralles, D. G., Nieto, R., McDowell, N. G., Dorigo, W. A., Verhoest, N. E. C., Liu, Y. Y., et al. (2016). Contribution of water-limited ecoregions to their own supply of rainfall. *Environmental Research Letters*, 11(12), 124007. Scopus. <https://doi.org/10.1088/1748-9326/11/12/124007>
- Mohamed, Y. A., van den Hurk, B. J. J. M., Savenije, H. H. G., & Bastiaanssen, W. G. M. (2005). Hydroclimatology of the Nile: Results from a regional climate model. *Hydrology and Earth System Sciences*, 9(3), 263–278. Scopus. <https://doi.org/10.5194/hess-9-263-2005>
- Monerie, P.-A., Biasutti, M., & Roucou, P. (2016). On the projected increase of Sahel rainfall during the late rainy season. *International Journal of Climatology*, 36(13), 4373–4383. Scopus. <https://doi.org/10.1002/joc.4638>
- Niang, C., Mancho, A. M., García-Garrido, V. J., Mohino, E., Rodríguez-Fonseca, B., & Curbelo, J. (2020). Transport pathways across the West African Monsoon as revealed by Lagrangian coherent structures. *Scientific Reports*, 10(1), 12543. <https://doi.org/10.1038/s41598-020-69159-9>
- Nicholson, S. E., Fink, A. H., & Funk, C. (2018). Assessing recovery and change in West Africa's rainfall regime from a 161-year record. *International Journal of Climatology*, 38(10), 3770–3786. <https://doi.org/10.1002/joc.5530>
- Nieto, R., Ciric, D., Vázquez, M., Liberato, M. L. R., & Gimeno, L. (2019). Contribution of the main moisture sources to precipitation during extreme peak precipitation months. *Advances in Water Resources*, 131, 103385. <https://doi.org/10.1016/j.advwatres.2019.103385>
- Nieto, R., Gimeno, L., & Trigo, R. M. (2006). A Lagrangian identification of major sources of Sahel moisture. *Geophysical Research Letters*, 33(18). <https://doi.org/10.1029/2006GL027232>
- Notaro, M., Wang, F., & Yu, Y. (2019). Elucidating observed land surface feedbacks across sub-Saharan Africa. *Climate Dynamics*, 53(3–4), 1741–1763. Scopus. <https://doi.org/10.1007/s00382-019-04730-3>
- Nouaceur, Z., & Murarescu, O. (2020). Rainfall variability and trend analysis of rainfall in West Africa (Senegal, Mauritania, Burkina Faso). *Water*, 12(6), 1754. <https://doi.org/10.3390/w12061754>
- O'Connor, J. C., Dekker, S. C., Staal, A., Tuinenburg, O. A., Rebel, K. T., & Santos, M. J. (2021). Forests buffer against variations in precipitation. *Global Change Biology*, 27(19), 4686–4696. <https://doi.org/10.1111/gcb.15763>

- Oguntunde, P. G., Abiodun, B. J., & Lischeid, G. (2016). A numerical modelling study of the hydroclimatology of the Niger River Basin, West Africa. *Hydrological Sciences Journal*, 61(1), 94–106. Scopus. <https://doi.org/10.1080/02626667.2014.980260>
- Otto, J., Raddatz, T., & Claussen, M. (2011). Strength of forest-albedo feedback in mid-Holocene climate simulations. *Climate of the Past*, 7(3), 1027–1039. <https://doi.org/10.5194/cp-7-1027-2011>
- Piao, S., Wang, X., Park, T., Chen, C., Lian, X., He, Y., et al. (2020). Characteristics, drivers and feedbacks of global greening. *Nature Reviews Earth & Environment*, 1(1), 14–27. <https://doi.org/10.1038/s43017-019-0001-x>
- Pokam, W. M., Djotang, L. A. T., & Mkankam, F. K. (2012). Atmospheric water vapor transport and recycling in Equatorial Central Africa through NCEP/NCAR reanalysis data. *Climate Dynamics*, 38(9), 1715–1729. <https://doi.org/10.1007/s00382-011-1242-7>
- Pranindita, A., Wang-Erlandsson, L., Fetzer, I., & Teuling, A. J. (2021). Moisture recycling and the potential role of forests as moisture source during European heatwaves. *Climate Dynamics*, 58(1–2), 609–624. <https://doi.org/10.1007/s00382-021-05921-7>
- Quesada, B., Devaraju, N., de Noblet-Ducoudré, N., & Arneeth, A. (2017). Reduction of monsoon rainfall in response to past and future land use and land cover changes. *Geophysical Research Letters*, 44(2), 1041–1050. Scopus. <https://doi.org/10.1002/2016GL070663>
- Sahlu, D., Moges, S. A., Nikolopoulos, E. I., Anagnostou, E. N., & Hailu, D. (2017). Evaluation of high-resolution multisatellite and reanalysis rainfall products over east Africa. *Advances in Meteorology*, 2017, 1–14. <https://doi.org/10.1155/2017/4957960>
- Salih, A. A. M., Zhang, Q., & Tjernström, M. (2015). Lagrangian tracing of Sahelian Sudan moisture sources. *Journal of Geophysical Research*, 120(14), 6793–6808. Scopus. <https://doi.org/10.1002/2015JD023238>
- Satgé, F., Defrance, D., Sultan, B., Bonnet, M.-P., Seyler, F., Rouché, N., et al. (2020). Evaluation of 23 gridded precipitation datasets across West Africa. *Journal of Hydrology*, 581, 124412. <https://doi.org/10.1016/j.jhydrol.2019.124412>
- Savenije, H. H. G. (1995). New definitions for moisture recycling and the relationship with land-use changes in the Sahel. *Journal of Hydrology*, 167(1–4), 57–78. [https://doi.org/10.1016/0022-1694\(94\)02632-L](https://doi.org/10.1016/0022-1694(94)02632-L)
- Schlesinger, W. H., & Jasechko, S. (2014). Transpiration in the global water cycle. *Agricultural and Forest Meteorology*, 189–190, 115–117. <https://doi.org/10.1016/j.agrformet.2014.01.011>
- Sodemann, H., Schwierz, C., & Wernli, H. (2008). Interannual variability of Greenland winter precipitation sources: Lagrangian moisture diagnostic and North Atlantic oscillation influence. *Journal of Geophysical Research*, 113(D3), D03107. <https://doi.org/10.1029/2007JD008503>
- Sorí, R., Nieto, R., Vicente-Serrano, S. M., Drummond, A., & Gimeno, L. (2017). A Lagrangian perspective of the hydrological cycle in the Congo River basin. *Earth System Dynamics*, 8(3), 653–675. <https://doi.org/10.5194/esd-8-653-2017>
- Sorí, R., Stojanovic, M., Nieto, R., Liberato, M. L. R., & Gimeno, L. (2022). Spatiotemporal variability of droughts in the Congo river basin. In *Congo basin hydrology, climate, and biogeochemistry* (pp. 187–203). American Geophysical Union (AGU). <https://doi.org/10.1002/9781119657002.ch11>
- Staal, A., Tuinenburg, O. A., Bosmans, J. H. C., Holmgren, M., van Nes, E. H., Scheffer, M., et al. (2018). Forest-rainfall cascades buffer against drought across the Amazon. *Nature Climate Change*, 8(6), 539–543. <https://doi.org/10.1038/s41558-018-0177-y>
- Sterling, S. M., Ducharne, A., & Polcher, J. (2013). The impact of global land-cover change on the terrestrial water cycle. *Nature Climate Change*, 3(4), 385–390. <https://doi.org/10.1038/nclimate1690>
- Stohl, A., Forster, C., Frank, A., Seibert, P., & Wotawa, G. (2005). Technical note: The Lagrangian particle dispersion model FLEXPART version 6.2. *Atmospheric Chemistry and Physics*, 5(9), 2461–2474. <https://doi.org/10.5194/acp-5-2461-2005>
- Stoy, P. C., El-Madany, T. S., Fisher, J. B., Gentine, P., Gerken, T., Good, S. P., et al. (2019). Reviews and syntheses: Turning the challenges of partitioning ecosystem evaporation and transpiration into opportunities. *Biogeosciences*, 16(19), 3747–3775. <https://doi.org/10.5194/bg-16-3747-2019>
- Te Wierik, S. A., Keune, J., Miralles, D. G., Gupta, J., Artzy-Randrup, Y. A., Gimeno, L., et al. (2022). Rainfall sources over African watersheds [Dataset]. <https://doi.org/10.6084/m9.figshare.1709988>
- Trenberth, K. E. (1999). Atmospheric moisture recycling: Role of advection and local evaporation. *Journal of Climate*, 12(5 II), 1368–1381. Scopus. [https://doi.org/10.1175/1520-0442\(1999\)012<1368:amrroa>2.0.co;2](https://doi.org/10.1175/1520-0442(1999)012<1368:amrroa>2.0.co;2)
- Tuinenburg, O. A., & Staal, A. (2020). Tracking the global flows of atmospheric moisture and associated uncertainties. *Hydrology and Earth System Sciences*, 24(5), 2419–2435. <https://doi.org/10.5194/hess-24-2419-2020>
- Tuinenburg, O. A., Theeuwens, J. J. E., & Staal, A. (2020). High-resolution global atmospheric moisture connections from evaporation to precipitation. *Earth System Science Data*, 12(4), 3177–3188. <https://doi.org/10.5194/essd-12-3177-2020>
- van der Ent, R. J., Wang-Erlandsson, L., Keys, P. W., & Savenije, H. H. G. (2014). Contrasting roles of interception and transpiration in the hydrological cycle—Part 2: Moisture recycling. *Earth System Dynamics*, 5(2), 471–489. <https://doi.org/10.5194/esd-5-471-2014>
- Van Der Ent, R. J., Savenije, H. H. G., Schaeffli, B., & Steele-Dunne, S. C. (2010). Origin and fate of atmospheric moisture over continents. *Water Resources Research*, 46(9). Scopus. <https://doi.org/10.1029/2010WR009127>
- Wada, Y., Van Beek, L. P. H., Van Kempen, C. M., Reckman, J. W. T. M., Vasak, S., & Bierkens, M. F. P. (2010). Global depletion of groundwater resources. *Geophysical Research Letters*, 37(20). Scopus. <https://doi.org/10.1029/2010GL044571>
- Wang, L., Good, S. P., & Caylor, K. K. (2014). Global synthesis of vegetation control on evapotranspiration partitioning. *Geophysical Research Letters*, 41(19), 6753–6757. <https://doi.org/10.1002/2014GL061439>
- Wang-Erlandsson, L., Fetzer, I., Keys, P. W., van der Ent, R. J., Savenije, H. H. G., & Gordon, L. J. (2018). Remote land use impacts on river flows through atmospheric teleconnections. *Hydrology and Earth System Sciences*, 22(8), 4311–4328. <https://doi.org/10.5194/hess-22-4311-2018>
- Wang-Erlandsson, L., van der Ent, R. J., Gordon, L. J., & Savenije, H. H. G. (2014). Contrasting roles of interception and transpiration in the hydrological cycle—Part 1: Temporal characteristics over land. *Earth System Dynamics*, 5(2), 441–469. <https://doi.org/10.5194/esd-5-441-2014>
- Washington, R., James, R., Pearce, H., Pokam, W. M., & Moufouma-Okia, W. (2013). Congo Basin rainfall climatology: Can we believe the climate models? *Philosophical Transactions of the Royal Society B: Biological Sciences*, 368(1625), 20120296. <https://doi.org/10.1098/rstb.2012.0296>
- Wei, Z., Yoshimura, K., Wang, L., Miralles, D. G., Jasechko, S., & Lee, X. (2017). Revisiting the contribution of transpiration to global terrestrial evapotranspiration. *Geophysical Research Letters*, 44(6), 2792–2801. <https://doi.org/10.1002/2016GL072235>
- Westra, S., Fowler, H. J., Evans, J. P., Alexander, L. V., Berg, P., Johnson, F., et al. (2014). Future changes to the intensity and frequency of short-duration extreme rainfall. *Reviews of Geophysics*, 52(3), 522–555. Scopus. <https://doi.org/10.1002/2014RG000464>
- Wierik, S. A. T., Cammeraat, E. L. H., Gupta, J., & Artzy-Randrup, Y. A. (2021). Reviewing the impact of land use and land use change on moisture recycling and precipitation patterns. *Water Resources Research*, e2020WR029234. <https://doi.org/10.1029/2020WR029234>
- Winkler, K., Fuchs, R., Rounsevell, M., & Herold, M. (2021). Global land use changes are four times greater than previously estimated. *Nature Communications*, 12(1), 2501. <https://doi.org/10.1038/s41467-021-22702-2>
- Worden, S., Fu, R., Chakraborty, S., Liu, J., & Worden, J. (2021). Where does moisture come from over the Congo Basin? *Journal of Geophysical Research: Biogeosciences*, 126(8), e2020JG006024. <https://doi.org/10.1029/2020JG006024>

- Yu, L., & Weller, R. A. (2007). Objectively analyzed air–sea heat fluxes for the global ice-free oceans (1981–2005). *Bulletin of the American Meteorological Society*, 88(4), 527–540. <https://doi.org/10.1175/BAMS-88-4-527>
- Yu, Y., Notaro, M., Wang, F., Mao, J., Shi, X., & Wei, Y. (2017). Observed positive vegetation-rainfall feedbacks in the Sahel dominated by a moisture recycling mechanism. *Nature Communications*, 8(1), 1873. Scopus. <https://doi.org/10.1038/s41467-017-02021-1>
- Zemp, D. C., Schleussner, C.-F., Barbosa, H. M. J., Van Der Ent, R. J., Donges, J. F., Heinke, J., et al. (2014). On the importance of cascading moisture recycling in South America. *Atmospheric Chemistry and Physics*, 14(23), 13337–13359. Scopus. <https://doi.org/10.5194/acp-14-13337-2014>
- Zeng, Z., Piao, S., Li, L. Z. X., Wang, T., Ciais, P., Lian, X., et al. (2018). Impact of Earth greening on the terrestrial water cycle. *Journal of Climate*, 31(7), 2633–2650. <https://doi.org/10.1175/JCLI-D-17-0236.1>
- Zhao, L., Liu, X., Wang, N., Kong, Y., Song, Y., He, Z., et al. (2019). Contribution of recycled moisture to local precipitation in the inland Heihe River Basin. *Agricultural and Forest Meteorology*, 271, 316–335. <https://doi.org/10.1016/j.agrformet.2019.03.014>
- Zipper, S. C., Keune, J., & Kollet, S. J. (2019). Land use change impacts on European heat and drought: Remote land-atmosphere feedbacks mitigated locally by shallow groundwater. *Environmental Research Letters*, 14(4), 044012. <https://doi.org/10.1088/1748-9326/ab0db3>